2016 Spring

# “Advanced Physical Metallurgy”

# - Bulk Metallic Glasses -

04.04.2016

Eun Soo Park

Office: 33-313
Telephone: 880-7221
Email: espark@snu.ac.kr
Office hours: by appointment

## 2.6 Methods to Synthesize Metallic Glasses

### 2.6.1 Vapor-state Processes: expensive & slow, electronic & magnetic applications

**Thermal Evaporation/ Sputtering/ Vapor Chemical Deposition**

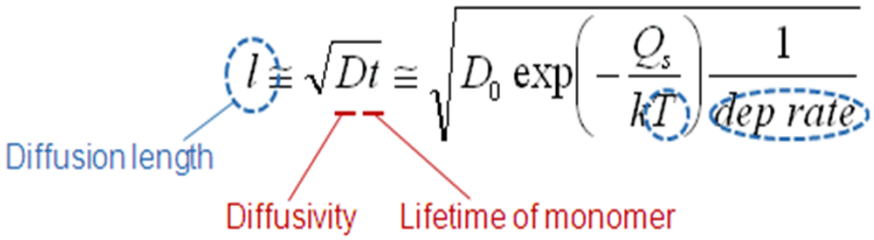


Deposition condition (T, dep rate) affects the diffusion length

Diffusion length determines the crystallinity of thin film

### 2.6.2 Liquid-state Processes : Rapid Solidification Process (RSP) $10^{5\text{-}6}$ K/s most ideal way to obtain metallic glasses, especially the bulk variety

**Splat Quenching/ Melt-spinning/ Electro Deposition/ Gas Atomization**

### 2.6.3 Solid-state Processes

**Mechanical Alloying & Milling/Hydrogen-induced Amorphization/ Multilayer Amorphization**_Solid state diffusional amorphization/ **Pressure-induced Amorphization/ Amorphization by Irradiation/ Severe Plastic Deformation**_Intense deformation at low temperatures/ **Accumulative Roll Bonding (ARB process)**

## 2.7 Bulk Metallic Glasses (BMGs)

- More commonly, metallic glasses with at least a diameter or section thickness of 1 mm are considered "bulk." (Nowadays researchers tend to consider 10 mm as the minimum diameter or section thickness at which a glass is designated bulk.)

### 2.7.1 Characteristics of Bulk Metallic Glasses

- The alloy systems have a minimum of three components; more commonly the number is much larger and that is why they are frequently referred to as multicomponent alloy systems.
- They can be produced at slow solidification rates, typically $10^3$ K $s^{-1}$ or less. The lowest solidification rate at which BMGs have been obtained was reported as 0.067 K $s^{-1}$, that is, 4 K $min^{-1}$ [61]; a really slow solidification rate indeed!
- BMGs exhibit large section thicknesses or diameters, a minimum of about 1 mm. The largest diameter of a bulk metallic glass rod produced till date is 72 mm in a $Pd_{40}Cu_{30}Ni_{10}P_{20}$ alloy [62].
- They exhibit a large supercooled liquid region. The difference between the glass transition temperature, $T_g$, and the crystallization temperature, $T_x$, that is, $\Delta T_x = T_x - T_g$, is large, usually a few tens of degrees, and the highest reported value so far is 131 K in a $Pd_{43}Ni_{10}Cu_{27}P_{20}$ alloy [17].

When the as-cast alloy is characterized by XRD techniques, the presence of a broad and diffuse peak is often taken to be evidence for the presence of a glassy phase. This is normally true. But, it should be realized that the technique of XRD is not very sensitive to the presence of a small volume fraction of a crystalline phase in a glassy phase, especially when the crystals are in nanocrystalline condition. Therefore, even if the XRD pattern shows a broad halo, the material may contain a small volume fraction of a crystalline phase dispersed in the glassy matrix. Further, a structure consisting of a glassy phase, or extremely fine grains, or a nanocrystalline material with a small grain size of about <10 nm, will all produce a broad and diffuse halo. Therefore, it is always desirable to confirm the lack of crystallinity in the material by conducting (high-resolution) transmission electron microscopy investigations.

## 2.7.2 The Origins of BMGs

# * History of Metallic Glasses

- **First amorphous metal produced by evaporation in 1934.**

  ** j. Kramer, Annalen der Phys. 1934; 19: 37.*

- **First amorphous alloy(CoP or NiP alloy)**

  **produced by electro-deposition in 1950.**

  ** A. Brenner, D.E. Couch, E.K. Williams, J. Res. Nat. Bur. Stand. 1950: 44; 109.*

- **First metallic glass ($Au_{80}Si_{20}$)**
  **produced by splat quenching at Caltech by Pol Duwez in 1957.**

  ** W. Klement, R.H. Willens, P. Duwez, Nature 1960; 187: 869.*

- **First bulk metallic glass ($Pd_{77.5}Cu_6Si_{16.5}$)**
  **produced by droplet quenching at Harvard Univ.**
  **by H.S. Chen and D. Turnbull in 1969**

  ** H.S. Chen and D. Turnbull, Acta Metall. 1969; 17: 1021.*

  **produced by water quenching of PdTMSi, Pt-Ni-P and Pd-Ni-P system**
  **by H.S. Chen in 1974 ( long glassy roads, 1-3 mm in diameter and several centimeters in length)**

  ** H.S. Chen, Acta Metall. 1974; 22: 1505*

## First bulk metallic glass: $Pd_{77.5}Cu_6Si_{16.5}$ ($T_{rg}$=0.64)

By droplet quenching (CR~800 K/s)

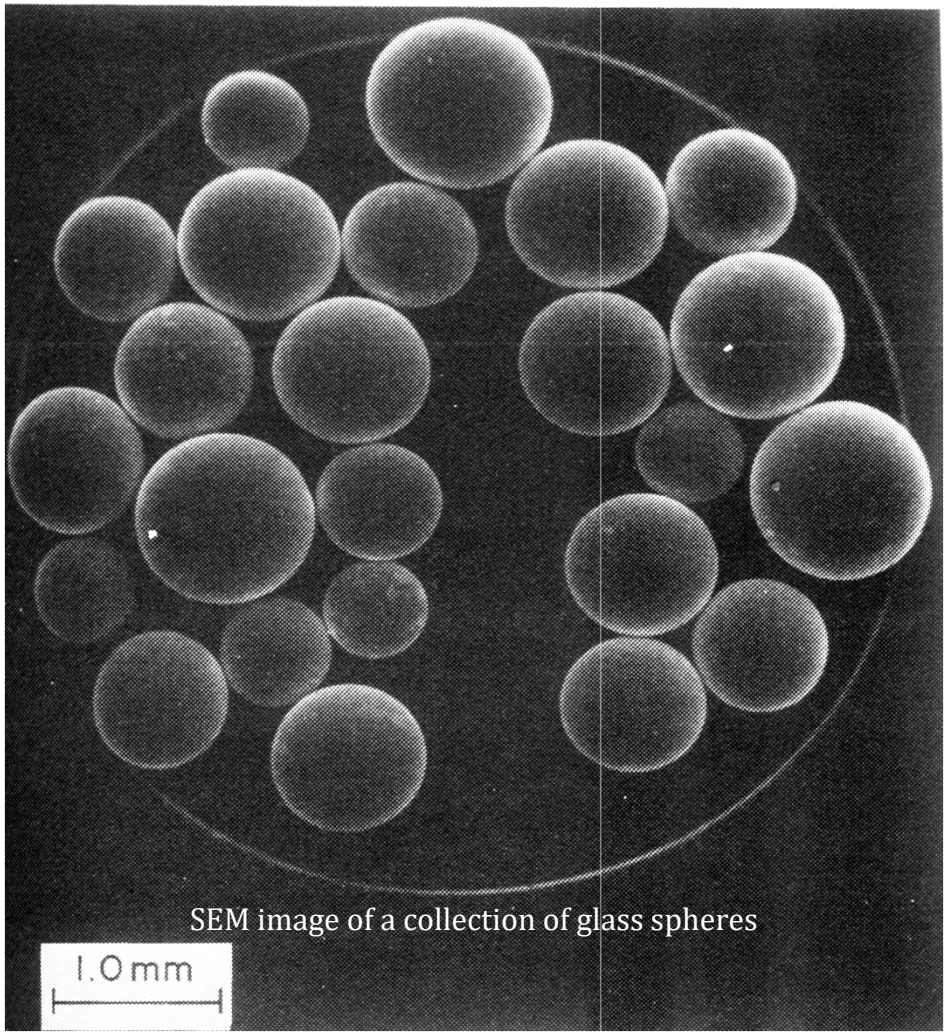


SEM image of a collection of glass spheres

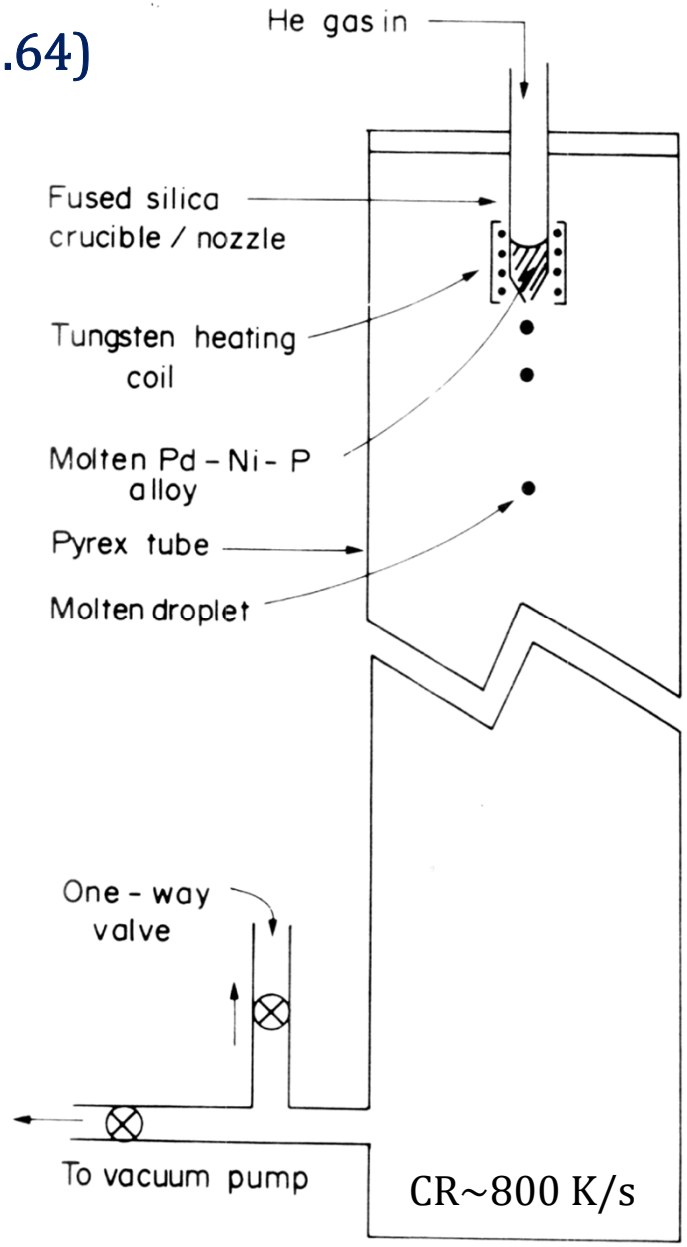


** H.S. Chen and D. Turnbull, Acta Metall. 1969; 17: 1021.*

# Bulk formation of a metallic glass: $Pd_{40}Ni_{40}P_{20}$

- **Alloy Selection: Consideration of $T_{rg}$**

  * $Pd_{82}Si_{18}$ ➡ $T_{rg}$=0.6
  - Homogeneous nucleation rate: >$10^5$/$cm^3$s
  - Critical cooling rate: > 800 K/s

  * $Pd_{77.5}Cu_6Si_{16.5}$ ➡ $T_{rg}$=0.64

  * $Pd_{40}Ni_{40}P_{20}$ ➡ $T_{rg}$=0.67
    $T_g$=590 K, $T_e$ = 880 K, $T_l$ = 985 K

<Schematic diagram of apparatus>

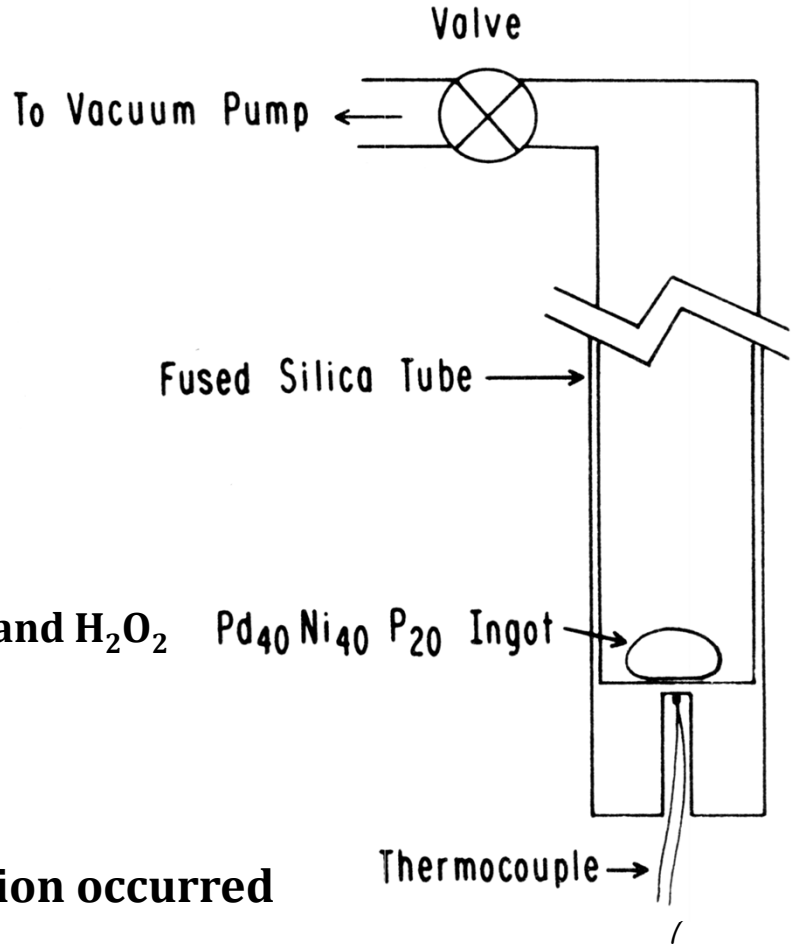


- **Suppression of Heterogeneous nucleation**

  1. **Surface Etching of ingot** in a mixture of HCL and $H_2O_2$
     : elimination of surface heterogeneities

  2. **Thermal cycling –5 cycles**
     : dissolution of nucleating heterogeneities
     ⟶ reduce the temperature at which nucleation occurred

# Bulk formation of a metallic glass: $Pd_{40}Ni_{40}P_{20}$

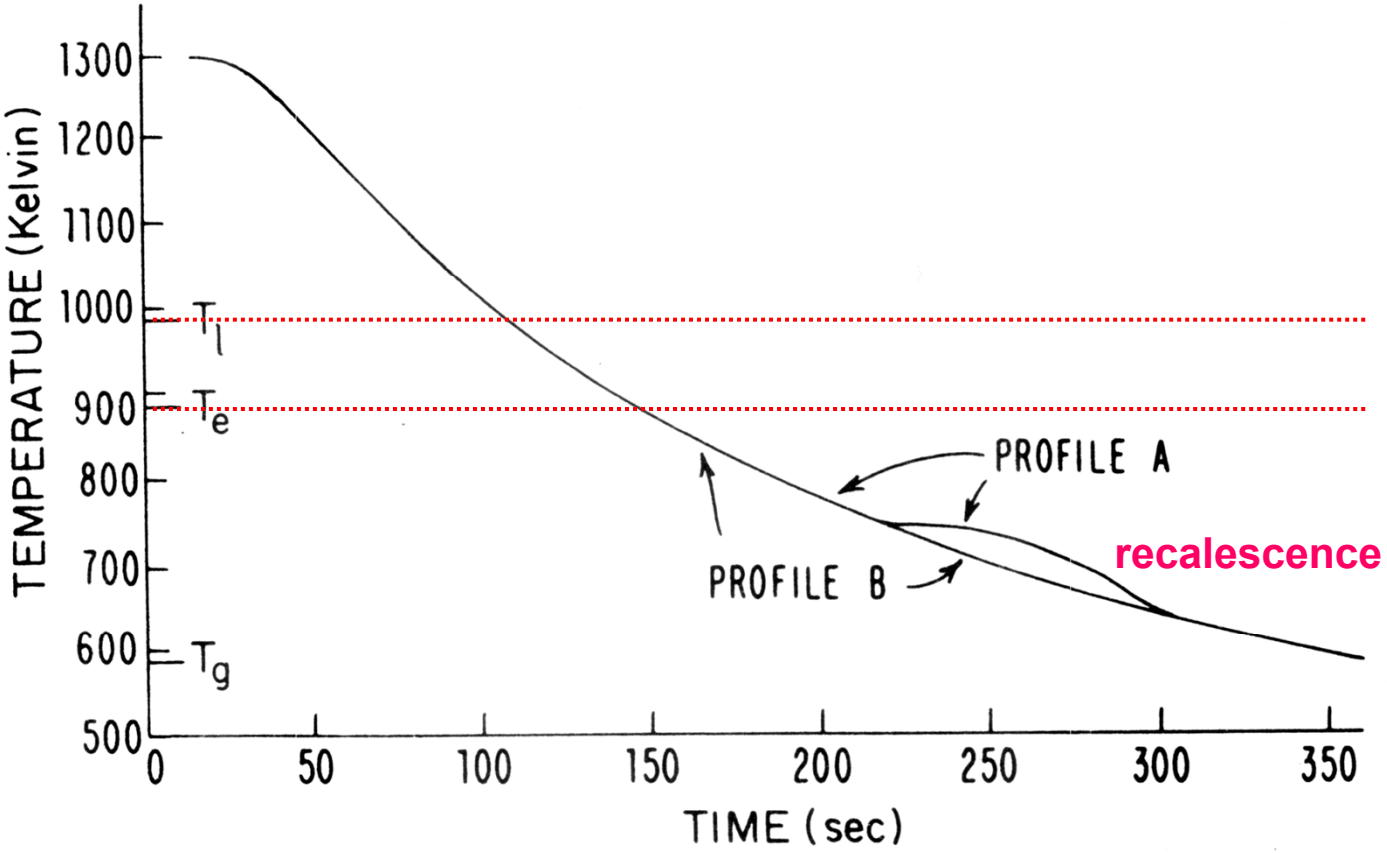


FIG. 2. Superposition of two cooling profiles: A—bulk crystallization which began at 740 K. B—formation of a glassy ingot.

*A.J. Drehman, A.L. Greer, D. Turnbull, Appl. Phys. Lett. 1982; 41: 716.*

# Bulk formation of a metallic glass: $Pd_{40}Ni_{40}P_{20}$

- **Largest ingot**

**- minimum dimension 0.6 cm and mass of 2.3 g**

**- Critical cooling rate: ~ 1.4 K/sec.**

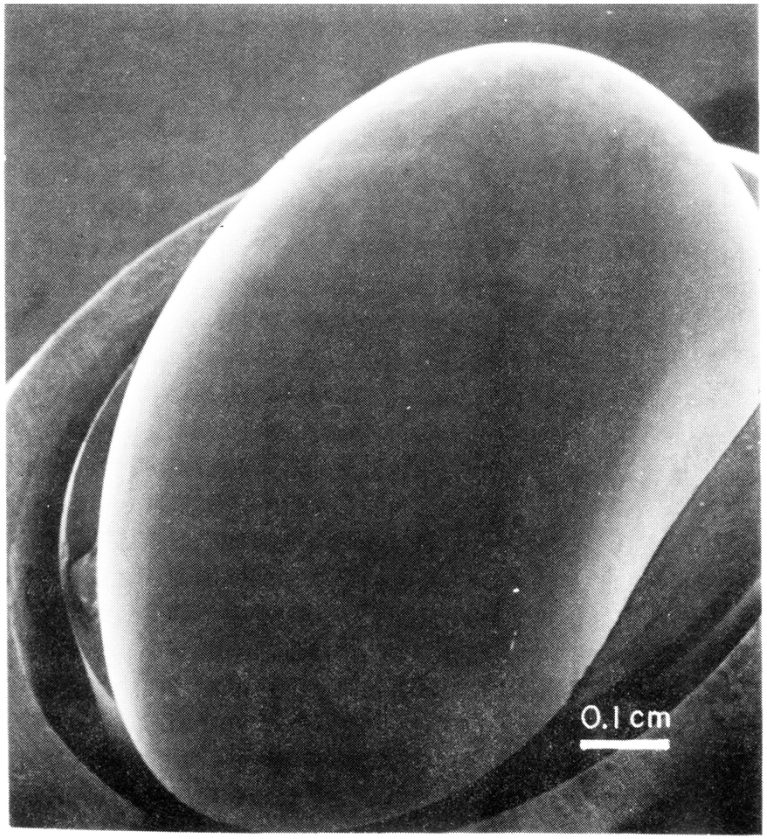


**Appl. Phys. Lett. 1982; 41: 716.*

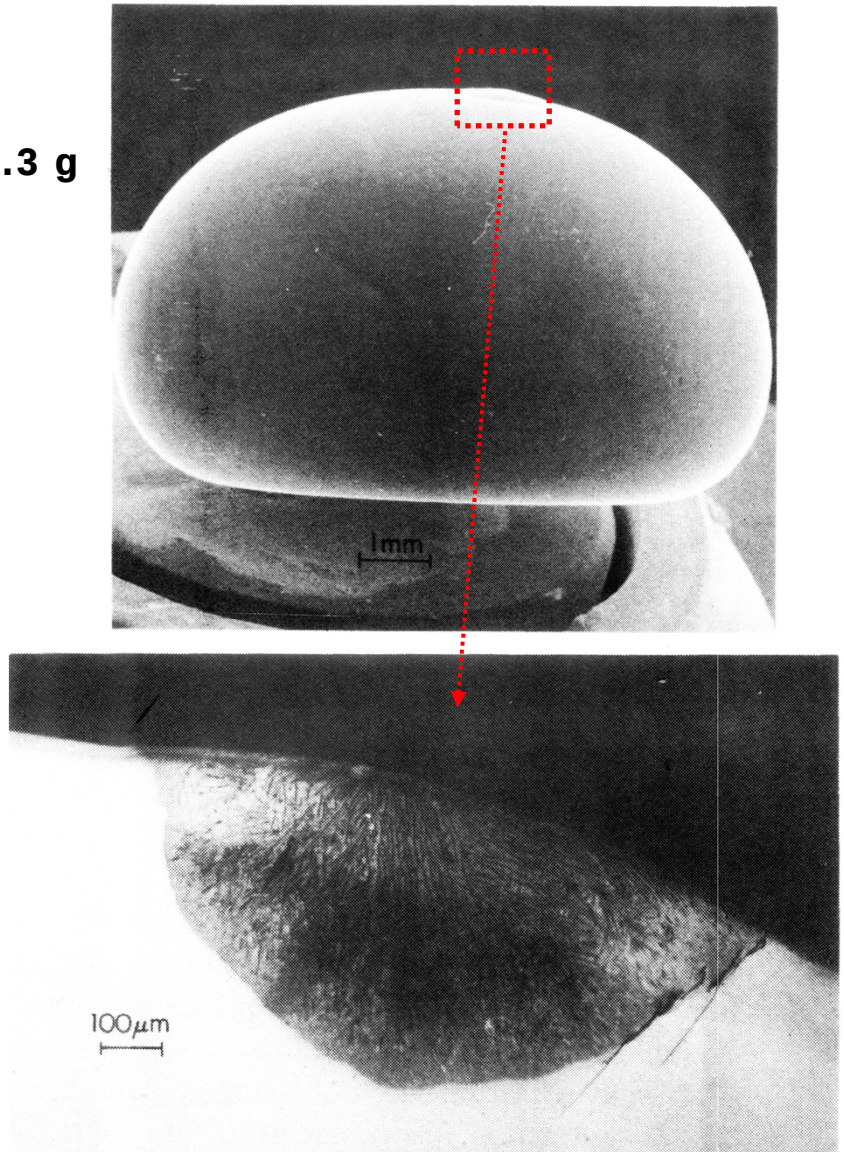


**OM image of the cross section of a crystalline inclusion showing the eutectic structure**

# Formation of bulk metallic glass by fluxing

- **Heterogeneous nucleation**

1. Surface oxide layer
2. Container walls
3. Motes in the liquid

➡ **Suppression**

1. **Ingot = Chemical etching**
   **by dilute aqua regia ($HNO_3$ + HCl)**
2. **Interior of the vessel = Cleaning**
   **by hydrofluoric acid**
3. **Impurities = Successive heating-cooling cycles in a molten oxide flux**

**$B_2O_3$ melting point 723 K, boiling point <40,000 K**

**After gravity segregation to the oxide-metal interface most heterophase impurities presumably are dissolved or deactivated (e.g., by being wet) by the molten oxide**

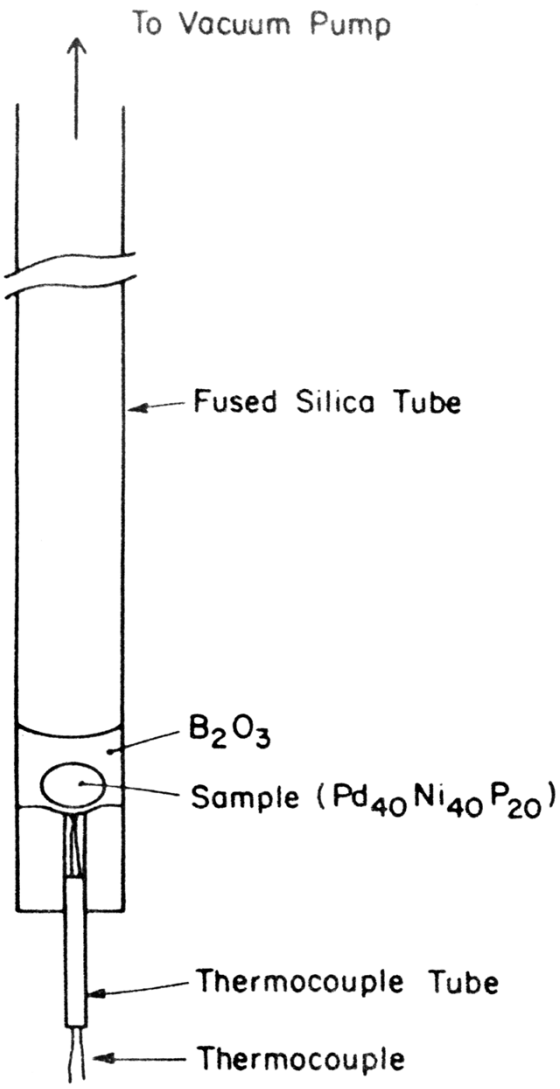

# Schematic process of fluxing

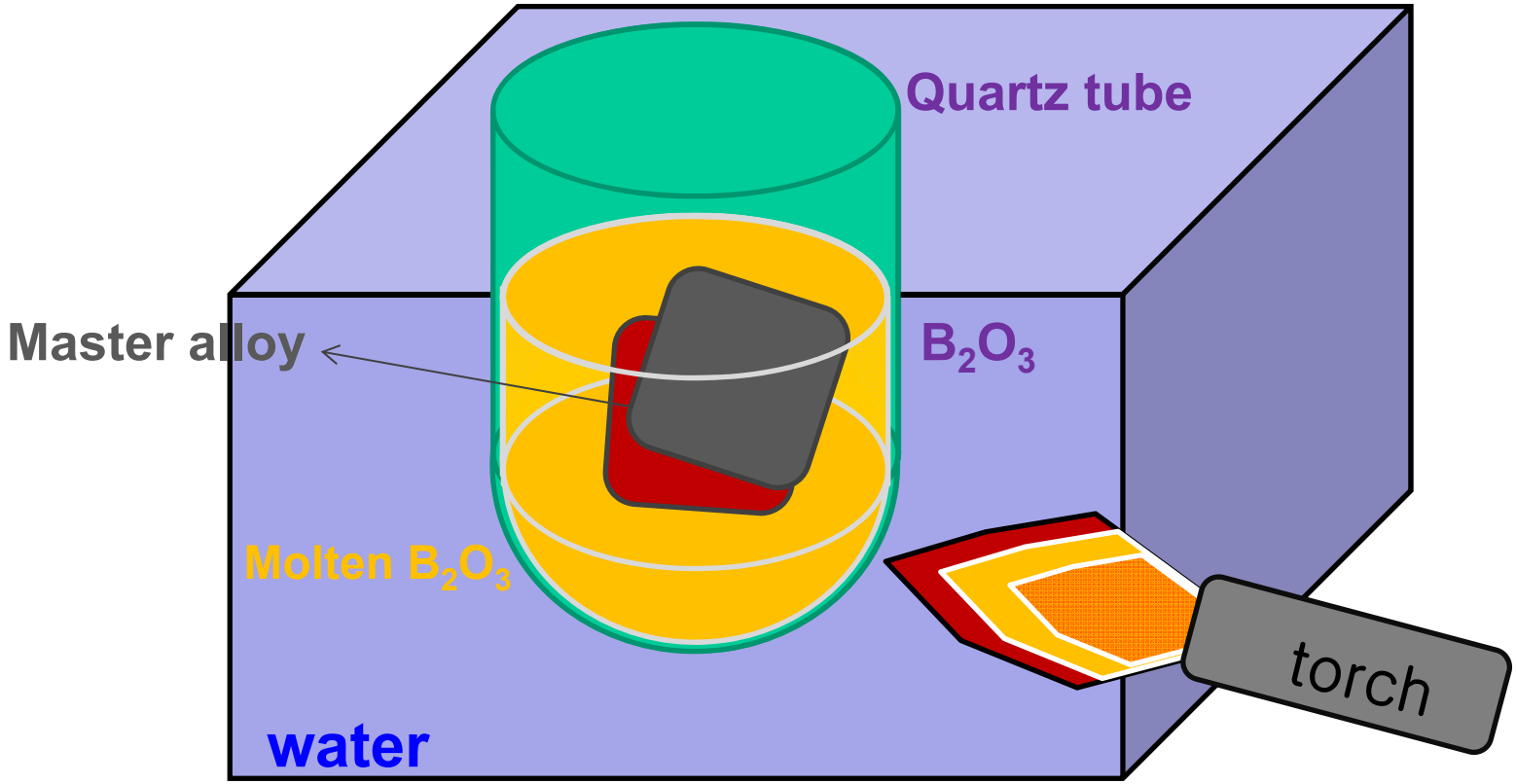


$B_2O_3$ melting point 723 K, boiling point <40,000 K

# Formation of centimeter-sized BMG by fluxing

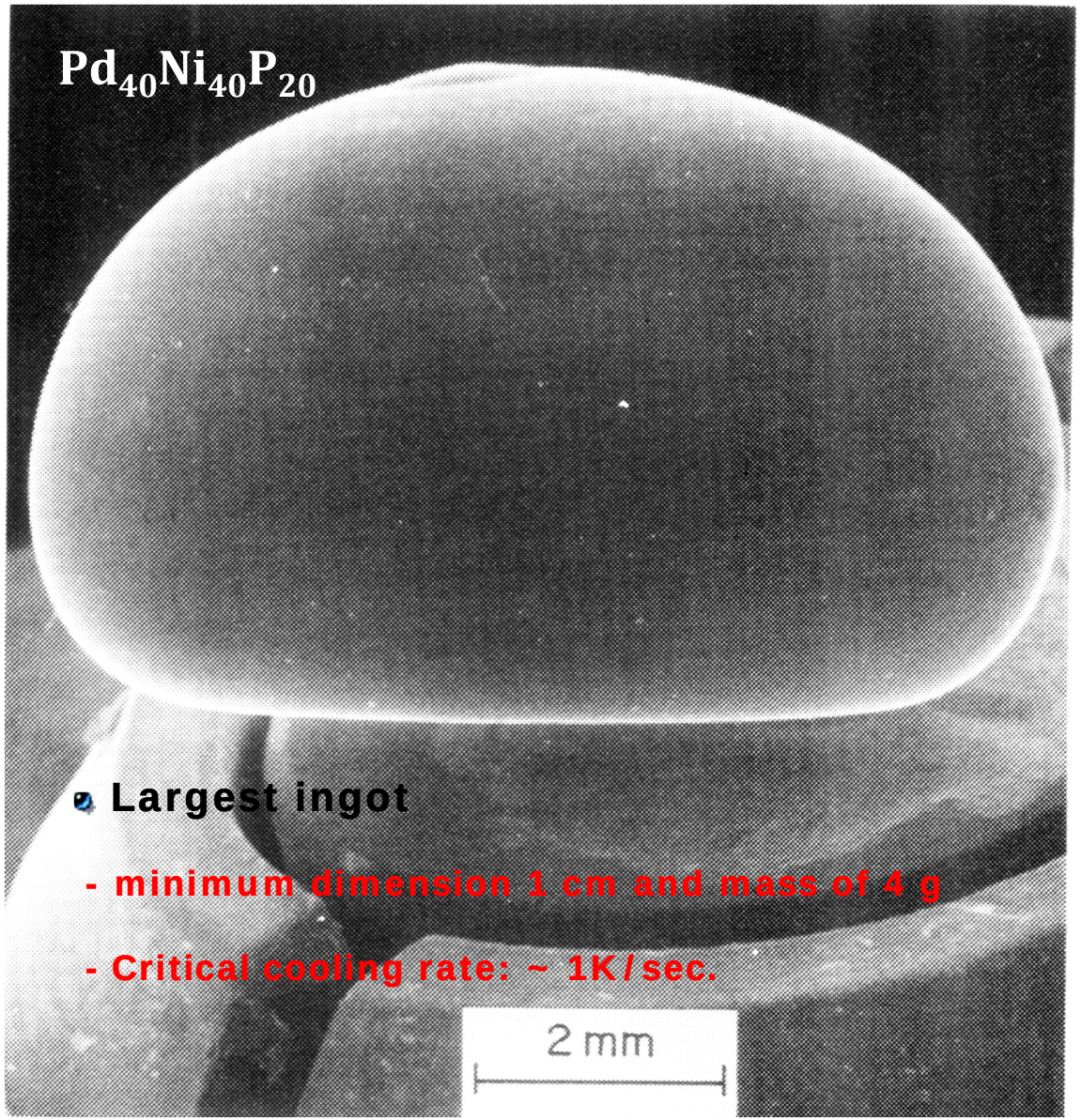

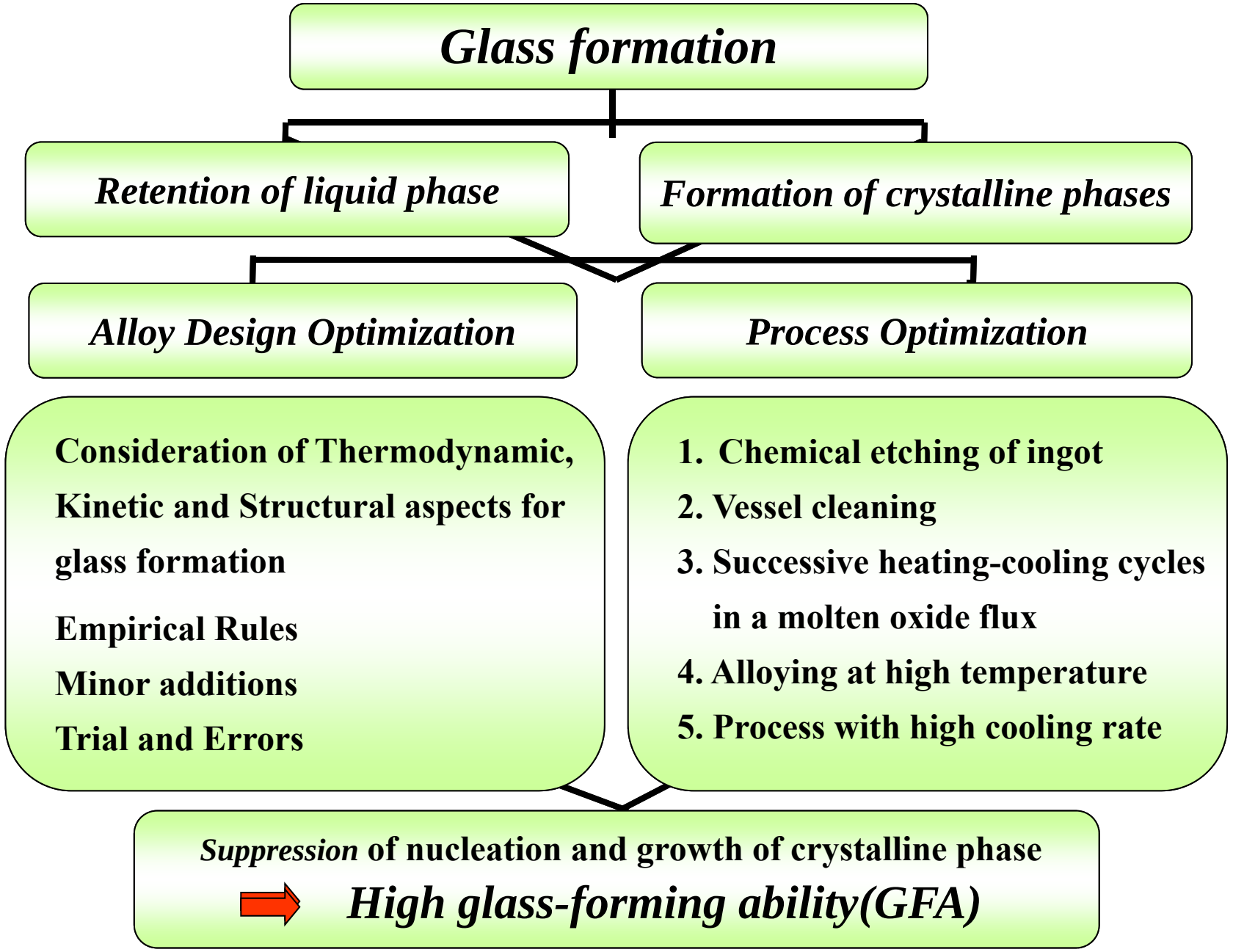
Glass formation
Retention of liquid phase
Formation of crystalline phases
Alloy Design Optimization
Process Optimization
Consideration of Thermodynamic, Kinetic and Structural aspects for glass formation
Empirical Rules
Minor additions
Trial and Errors
1. Chemical etching of ingot
2. Vessel cleaning
3. Successive heating-cooling cycles in a molten oxide flux
4. Alloying at high temperature
5. Process with high cooling rate
Suppression of nucleation and growth of crystalline phase
High glass-forming ability(GFA)

# Formation of centimeter-sized BMG by fluxing

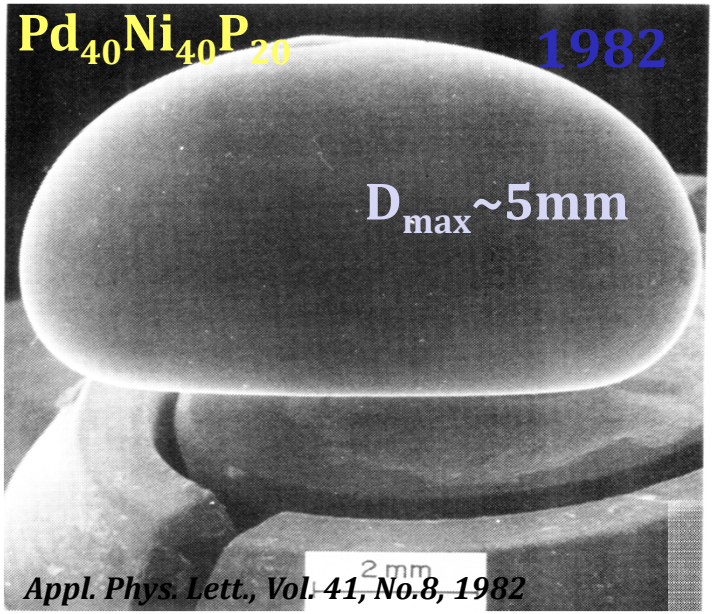


1984

$D_{max}$~10mm

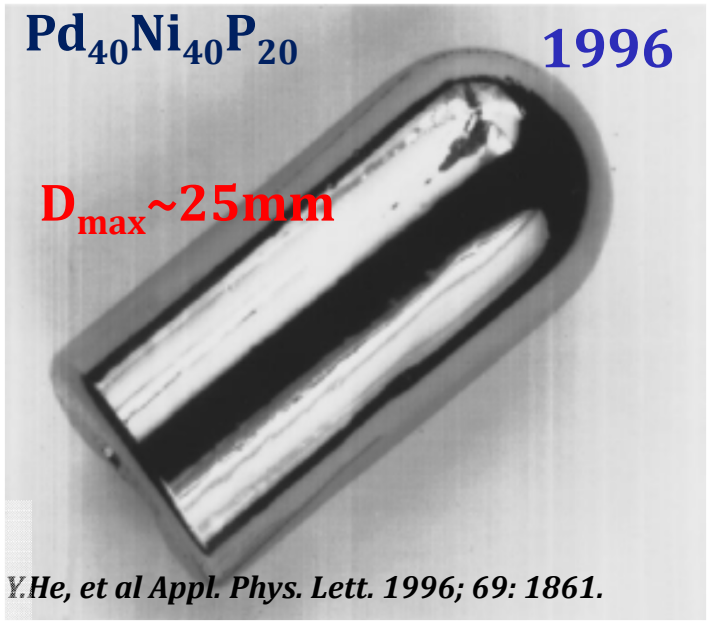


**After fluxing treatment**

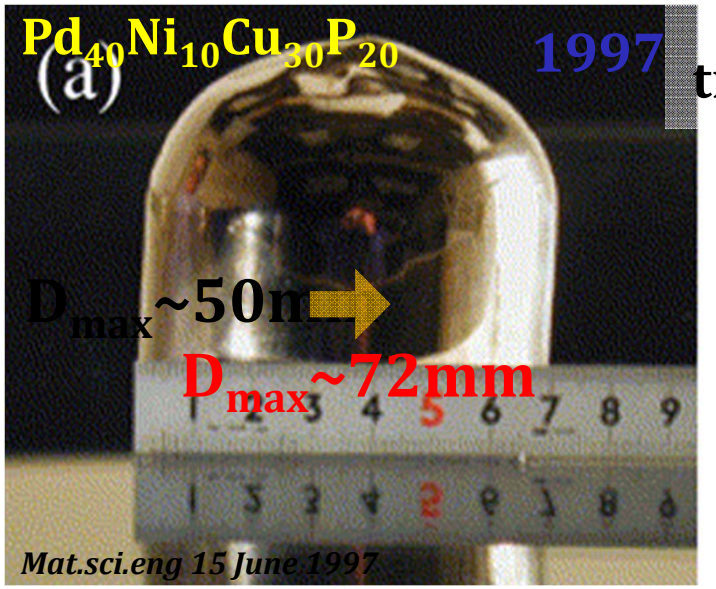


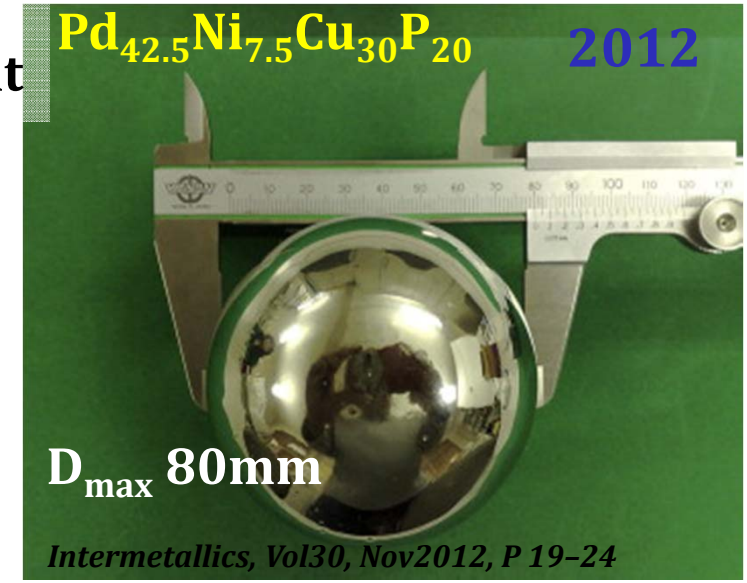

Starting in the late 1980s, the RSP group at Tohoku University in Sendai, Japan, has systematically investigated the glass-forming ability (GFA) of different alloy systems and was able to produce bulk glassy alloys in some of the systems at solidification rates of $10^3$ K $s^{-1}$ or lower. A brief account of the development of BMGs at Tohoku University is described below.

Al–La–Ni [67] and Mg–Ni–La [68] glassy alloys were produced in a wide composition range → The $\Delta T_x$ values reported were 69 K for the $La_{55}Al_{25}Ni_{20}$ glass and 58 K for the $Mg_{50}Ni_{30}La_{20}$ glass. These $\Delta T_x$ values are much larger than those reported for the noble-metal-based glasses, Pd–Ni–P and $Pt_{60}Ni_{15}P_{25}$ (35–40 K) reported earlier.

## Figure 2.6

**X-ray diffraction patterns of La55Al25Ni20 glassy samples in the water-quenched rod (0.8 mm dia. → Dmax = 1.2 mm) and melt-spun ribbon (20μm) conditions. Note that in both the cases, the diffraction pattern shows only a broad peak and sharp peaks indicative of any crystalline phase are absent. Furthermore, the position of the broad peak is the same in both the samples, suggesting that the glassy phase produced in same in both the cases.**

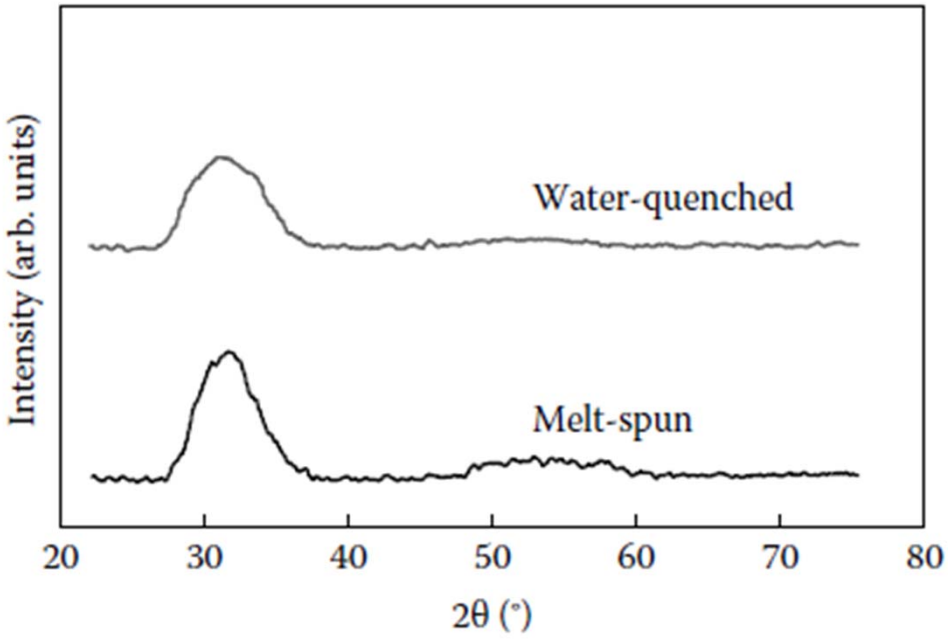


** Inoue A, et al., Mater. Trans. JIM, 30, 722, 1989.*

These observations have subsequently been confirmed in a number of other alloy systems and by several researchers. Subsequent to this initial discovery, Peker and Johnson [70] produced a 14 mm diameter fully glassy rod in the composition $Zr_{41.2}Ti_{13.8}Cu_{12.5}Ni_{10.0}Be_{22.5}$ (most commonly referred to as Vitreloy 1 or Vit 1, and now redesignated as liquid metal or LM-001), and since then there has been an explosion in the research activity in this area all over the world.

**A highly processable metallic glass: $Zr_{41.2}Ti_{13.8}Cu_{12.5}Ni_{10.0}Be_{22.5}$**

A. Peker and W. L. Johnson
*W. M. Keck Laboratory of Engineering Materials, California Institute of Technology, Pasadena, California 91125*

We report on the properties of one example of a new family of metallic alloys which exhibit excellent glass forming ability. The critical cooling rate to retain the glassy phase is of the order of 10 K/s or less. Large samples in the form of rods ranging up to 14 mm in diameter have been prepared by casting in silica containers.

* ***Appl. Phys. Lett. 63: 2342-2344.***

Starting with the initial discovery of the formation of BMGs in the La–Al–Ni system, the Tohoku group has produced a very large number of BMGs in different alloy systems based on Mg, Zr, Ti, Pd, Fe, Co, Ni, and Cu. They have been able to produce several new alloys in the BMG state and also increase the critical (or maximum) diameter of the BMG alloy rods during the last nearly 20 years.

# Recent BMGs with critical size ≥ 10 mm

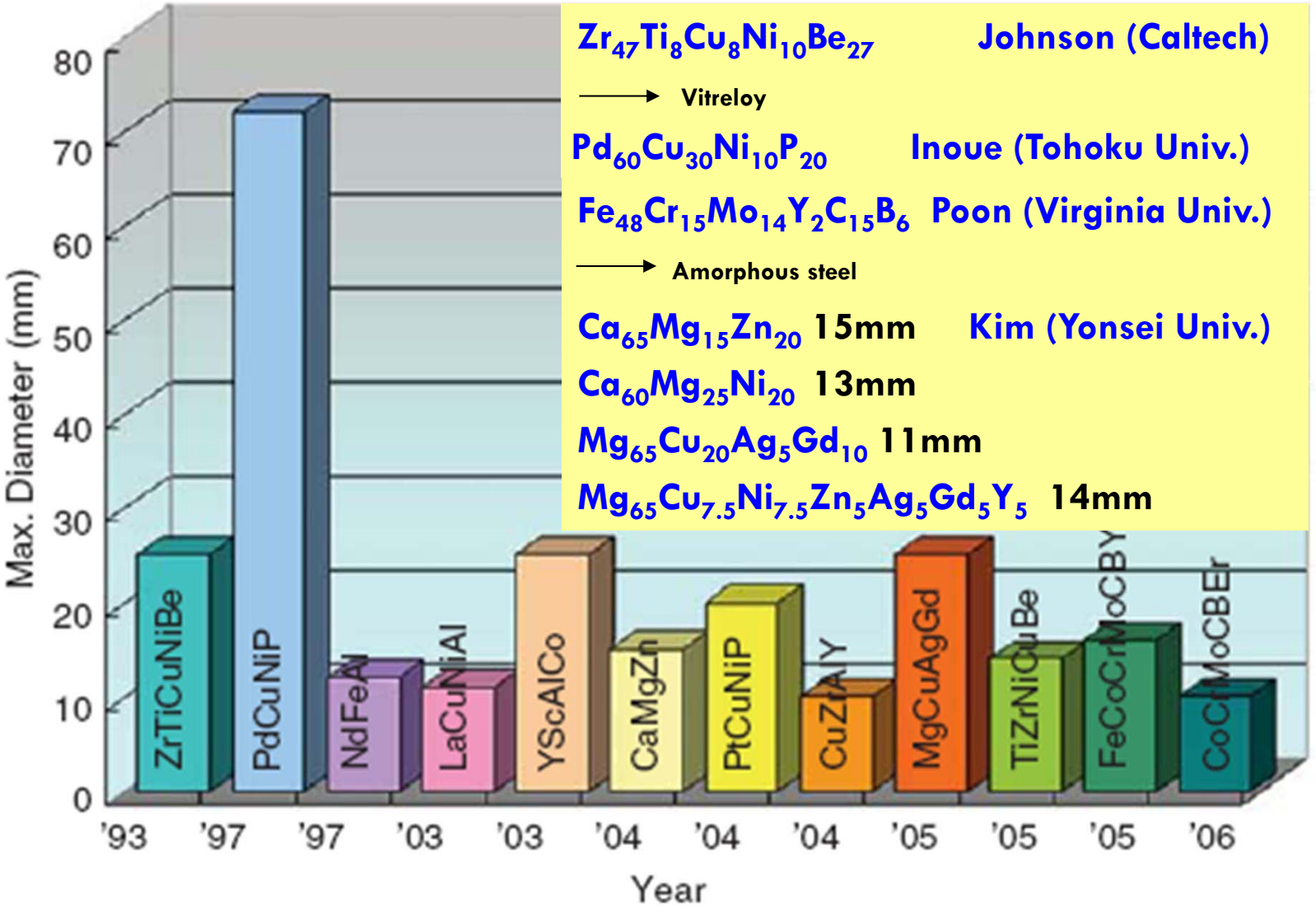

# Bulk glass formation in the Pd-/Ni-/Cu-/Zr- element system

**Massy Ingot Shape**

(a) Pd-Cu-Ni-P

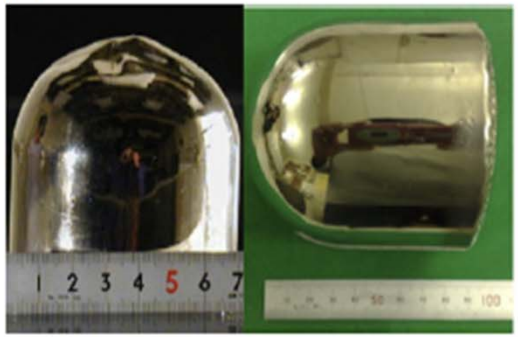

72ϕx 75 mm 80ϕx 85 mm

(b) Zr-Al-Ni-Cu

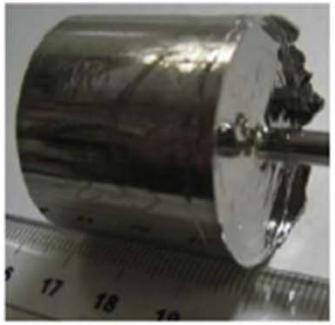

(c) Cu-Zr-Al-Ag

(d) Ni-Pd-P-B

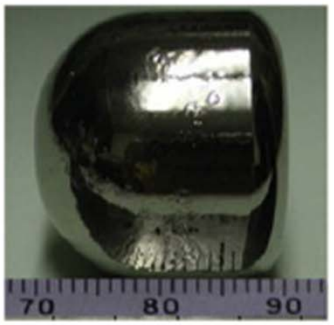

**Cylindrical Rods**

(e) Pd-Cu-Ni-P

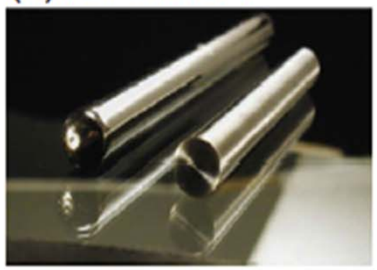

(f) Pt-Pd-Cu-P

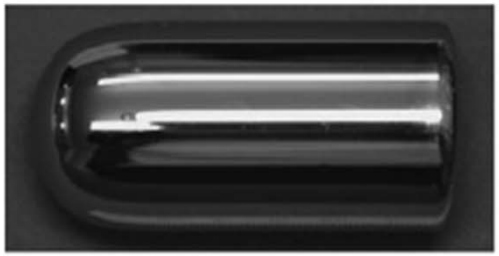

**Hollow Pipes**

(g) Pd-Cu-Ni-P

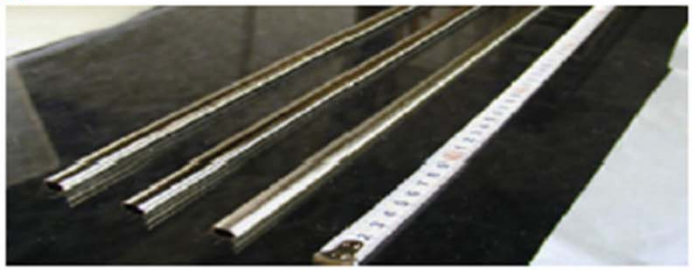

# Recent BMGs with critical size ≥ 10 mm

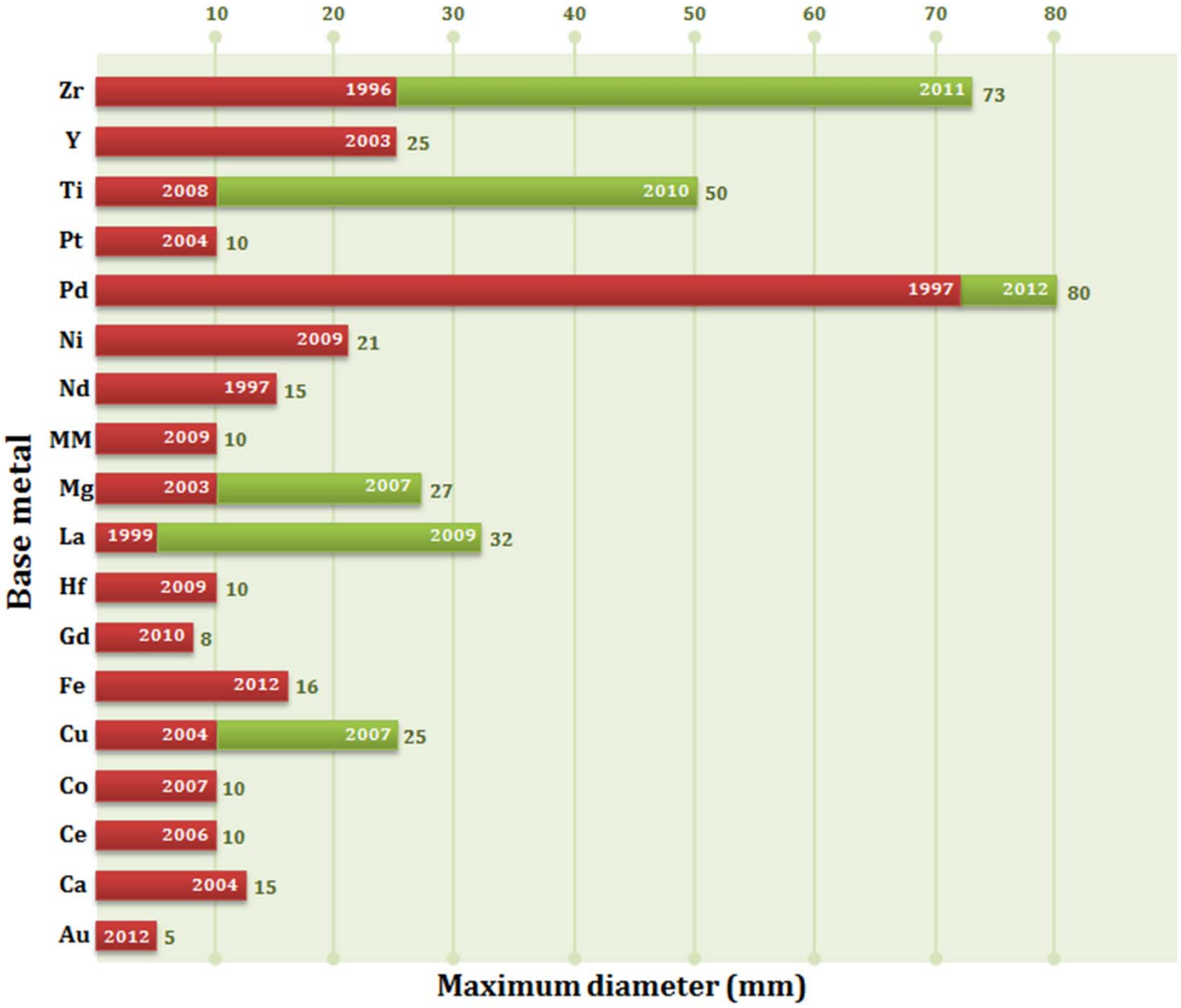

# 3. Glass-Forming Ability of Alloys

- **Many glasses were produced more or less by trial and error.**

  **→ The ability of a metallic alloy to transform into the glassy state is defined in this chapter as the glass-forming ability (GFA).**

## 3.2 Critical Cooling Rate

If an alloy melt is solidified from a temperature above the liquidus temperature, $T_l$ to below the glass transition temperature, $T_g$, then the volume fraction of the solid crystalline phase, $X$ formed under non-isothermal crystallization conditions can be given by the equation [8,9]

$$X(T) = \frac{4\pi}{3R^4} \int_{T_l}^{T_g} I(T') \left[ \int_{T''}^{T_g} U(T'')dT'' \right]^3 dT' \qquad (3.1)$$

where $I$ and $U$ are the steady-state nucleation frequency and crystal growth rate,

$X = 10^{-6}$ →

$$R_c^4 = \frac{4\pi}{3\times 10^{-6}} \int_{T_l}^{T_g} I(T') \left[ \int_{T''}^{T_g} U(T'')dT'' \right]^3 dT' \qquad (3.2)$$

Since the equations for $I$ and $U$ contain terms like viscosity of the supercooled liquid, $\eta$, entropy of fusion, $\Delta S_f$, etc., the critical cooling rate, $R_c$ decreases with increasing $\eta$, $\Delta S_f$, and decreasing liquidus temperature, $T_l$. The best way to experimentally determine $R_c$ is by constructing the time–temperature–transformation ($T$–$T$–$T$) diagrams.

## 3.2.1 T-T-T Diagrams: isothermal processes

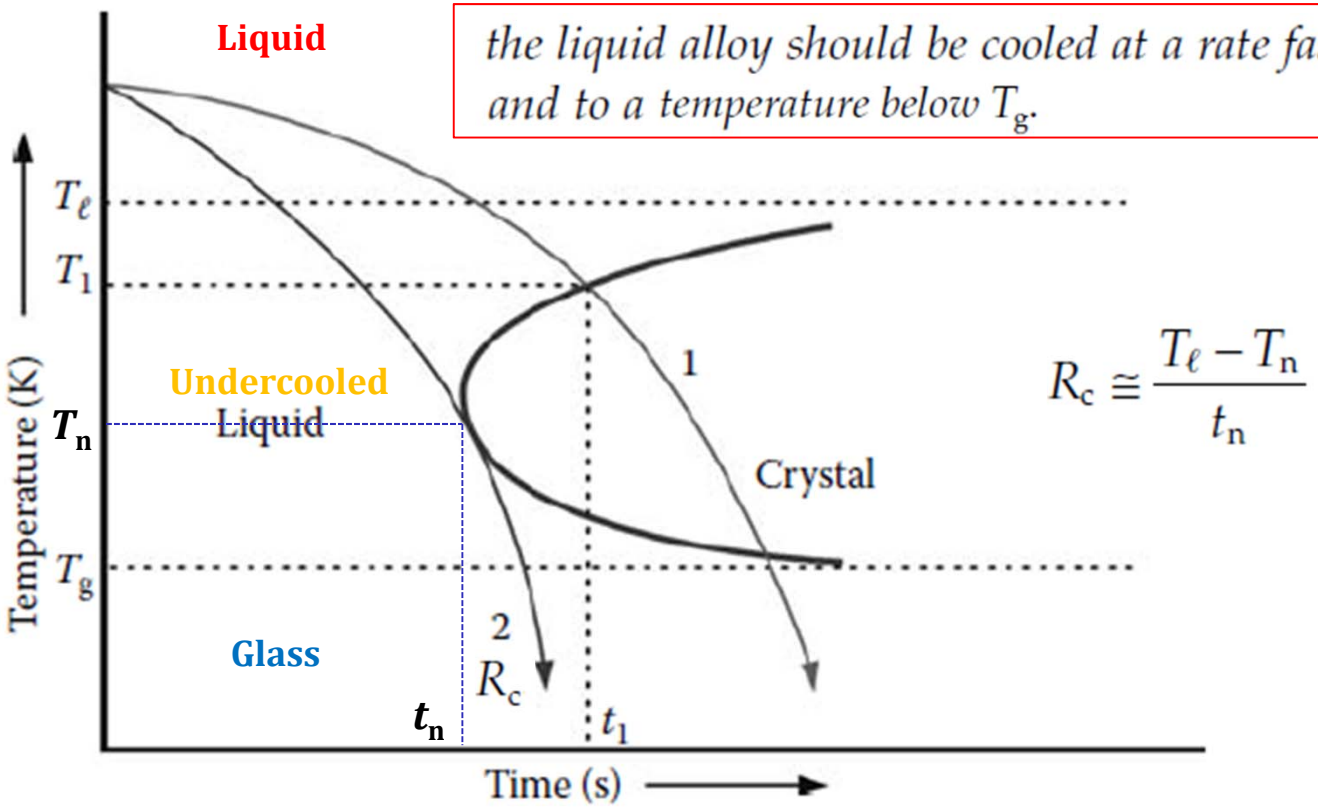


**FIGURE 3.1**
Schematic time–temperature–transformation (*T–T–T*) diagram for a hypothetical alloy system. When the liquid alloy is cooled from above the liquidus temperature $T_\ell$, at a rate indicated by curve "1," solidification starts at a temperature $T_1$ and time $t_1$. The resultant product is a crystalline solid. However, if the same liquid alloy is now cooled, again from $T_\ell$, at a rate faster than the rate indicated by curve "2," the liquid will continue to be in the undercooled state, and when cooled below the glass transition temperature $T_g$, the liquid is "frozen-in" and a glassy phase is formed. The cooling rate represented by curve "2" is referred to as the critical cooling rate, $R_c$.

# $R_c$ vs $D_{max}$ in Ti-Zr-Cu-Ni alloy system

J. Appl. Phys. 78, 1 December 1995

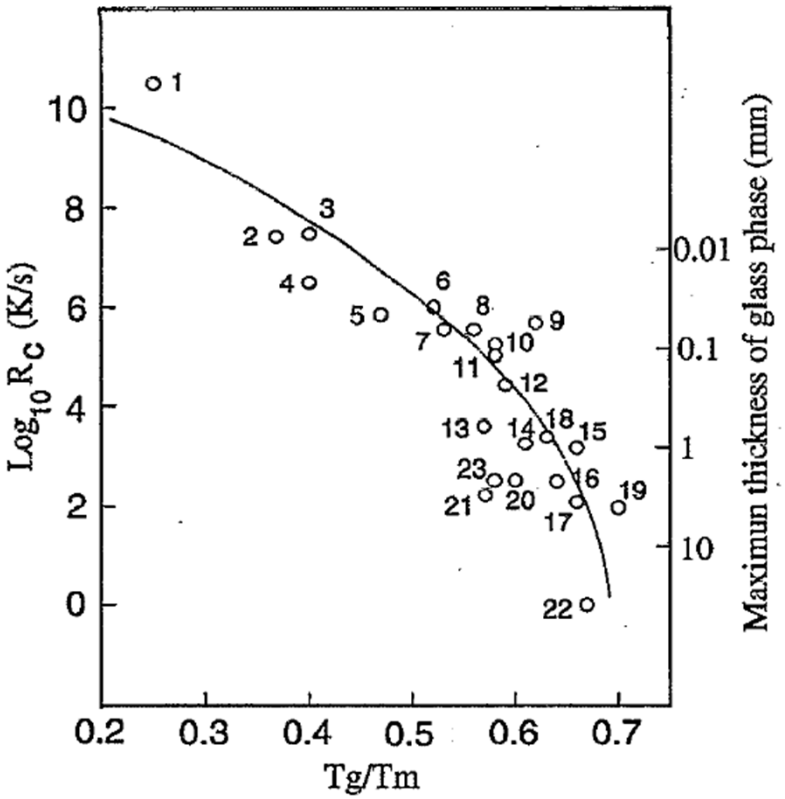


FIG. 1. Critical cooling rates for glass formation and corresponding maximum thickness of glass phase. Key to the alloys: (1) Ni; (2) $Fe_{91}B_9$; (3) $Fe_{89}B_{11}$; (4) Te; (5) $Au_{77.8}Ge_{13.8}Si_{8.4}$; (6) $Fe_{83}B_{17}$; (7) $Fe_{41.5}Ni_{41.5}B_{17}$; (8) $Co_{75}Si_{15}B_{10}$; (9) Ge; (10) $Fe_{79}Si_{10}B_{11}$; (11) $Ni_{75}Si_8B_{17}$; (12) $Fe_{80}P_{13}C_7$; (13) $Pt_{60}Ni_{15}P_{25}$; (14) $Pd_{82}Si_{18}$; (15) $Ni_{62.4}Nb_{37.6}$; (16) $Pd_{77.5}Cu_6Si_{16.5}$; (17) $Pd_{40}Ni_{40}P_{20}$ (above from Ref. 3); (18) $Au_{55}Pb_{22.5}Sb_{22.5}$ (Ref. 6); (19) $La_{55}Al_{25}Ni_{10}Cu_{10}$ (Ref. 7); (20) $Mg_{65}Cu_{25}Y_{10}$ (Ref. 8); (21) $Zr_{65}Cu_{17.5}Ni_{10}Al_{7.5}$ (Ref. 9); (22) $Zr_{41.2}Ti_{13.8}Cu_{12.5}Ni_{10}Be_{22.5}$ (Refs. 4 and 5); (23) $Ti_{34}Zr_{11}Cu_{47}Ni_8$.

**Total cooling time $\tau \sim (R^2/\kappa)$**

**sample dimension (dia. or thickness) : R**

**initial temperature: $T_m$**

**thermal diffusivity : $\kappa$**

**$\kappa = K/C$**

**thermal conductivity : K**

**heat capacity per unit volume: C**

$$\dot{T} = \frac{dT}{dt} = \frac{(T_m - T_g)}{\tau} = \frac{K(T_m - T_g)}{CR^2}$$

**For Ti-Zr-Cu-Ni system,**

**$T_m$-$T_g$ ~400K  K~0.1W/cm $s^{-1}K^{-1}$  C~4J/$cm^3K^{-1}$**

$$\dot{T}(\mathrm{K/s}) = 10/R^2(\mathrm{cm})$$

## 3.2.2. Effect of Alloying Elements

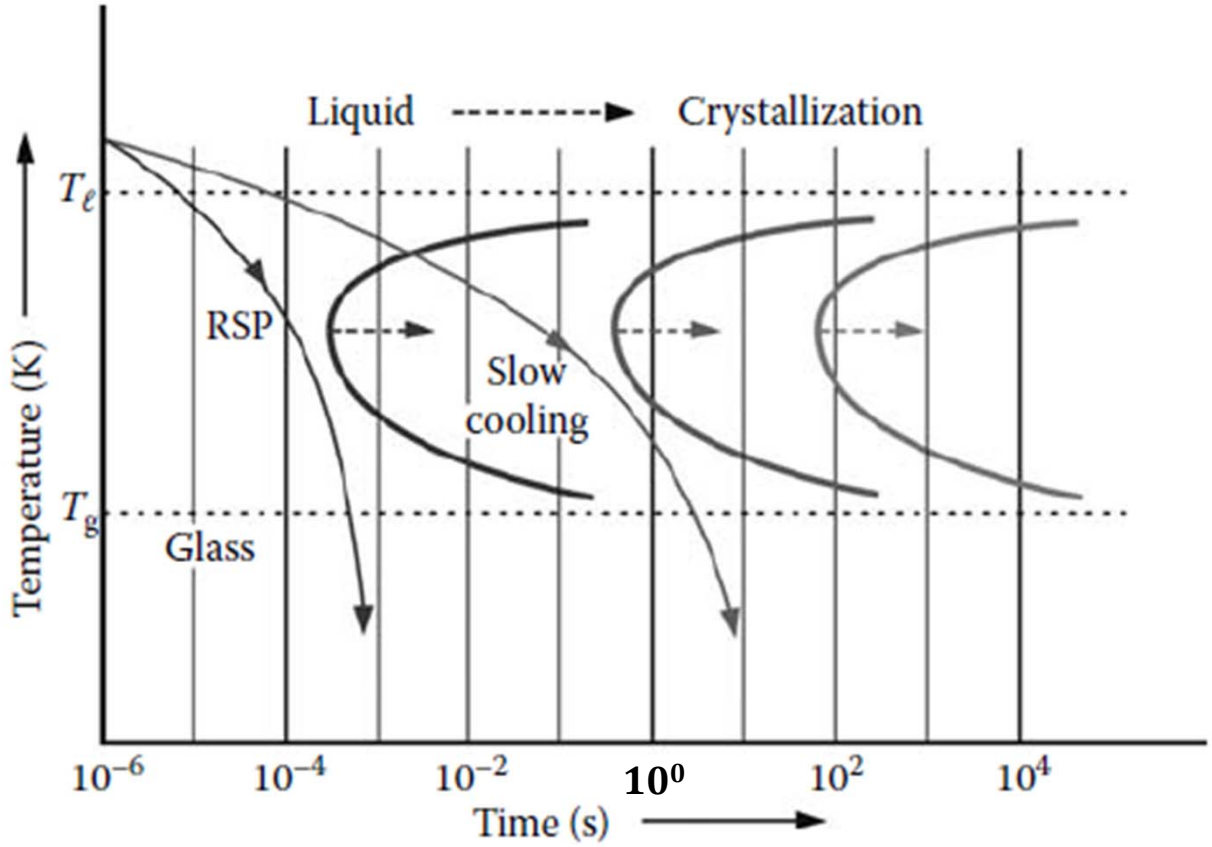


**FIGURE 3.2**
Position of the *T–T–T* curves with the addition of a large number of alloying elements. The *C*-curve shifts to the right with increasing number of alloying elements and consequently, the glassy phase can be synthesized at slow solidification rates. The left-most *C*-curve represents a typical situation of an alloy system where a glassy phase is obtained by rapid solidification processing (RSP) from the liquid state. The middle *C*-curve represents an alloy composition where a glassy phase can be obtained by slow cooling. The right-most *C*-curve represents a situation when an alloy can be very easily produced in a glassy state.

## $R_c$

| $> 10^{10\text{-}12}$ K/s | $10^{4\text{-}6}$ K/s | $10^{2}$ K/s | $1.3\text{x}10^{-2}$ or 0.067K/s | $10^{-5}$ to $10^{-4}$ K/s |
|---|---|---|---|---|
| pure metals | binary metallic liquids | typically multicomponent | $Pd_{37.5}Cu_{32.5}Ni_{10}P_{20}$ <br> $Pd_{30}Pt_{17.5}Cu_{32.5}P_{20}$ | Oxide glasses |

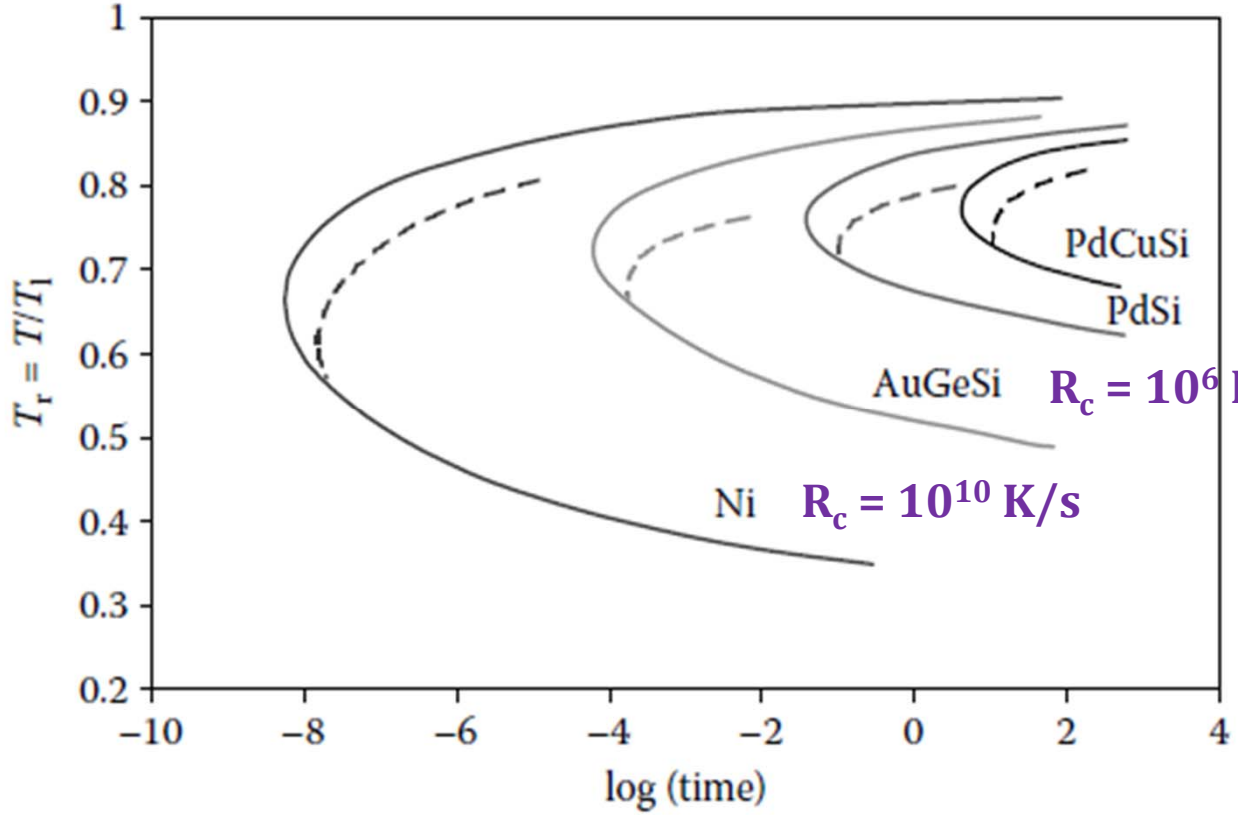


$$R_c = \frac{\Delta T}{t_n}$$

PdCuSi $R_c = 3.5\text{x}10^{1}$ K/s

PdSi $R_c = 3\text{x}10^{3}$ K/s

AuGeSi $R_c = 10^{6}$ K/s

Ni $R_c = 10^{10}$ K/s

**FIGURE 2.3**
Time–temperature–transformation (*T–T–T*) curves (solid lines) and the corresponding continuous cooling transformation curves (dashed lines) for the formation of a small volume fraction for pure metal Ni, and $Au_{78}Ge_{14}Si_{8}$, $Pd_{82}Si_{18}$, and $Pd_{78}Cu_{6}Si_{16}$ alloys.

| $T_{rg}$ | | 1/4 | 1/2 | 2/3 |
|---|---|---|---|---|

### 3.2.3 Measurement of $R_c$

The measurement of $R_c$ is an involved and time-consuming process. One has to take a liquid alloy of a chosen composition and allow it to solidify at different cooling rates and determine the nature and amount of phases formed after solidification.

## Measurement of $R_c$ in $Ca_{65}Mg_{15}Zn_{20}$ ($D_{max}$>15 mm)

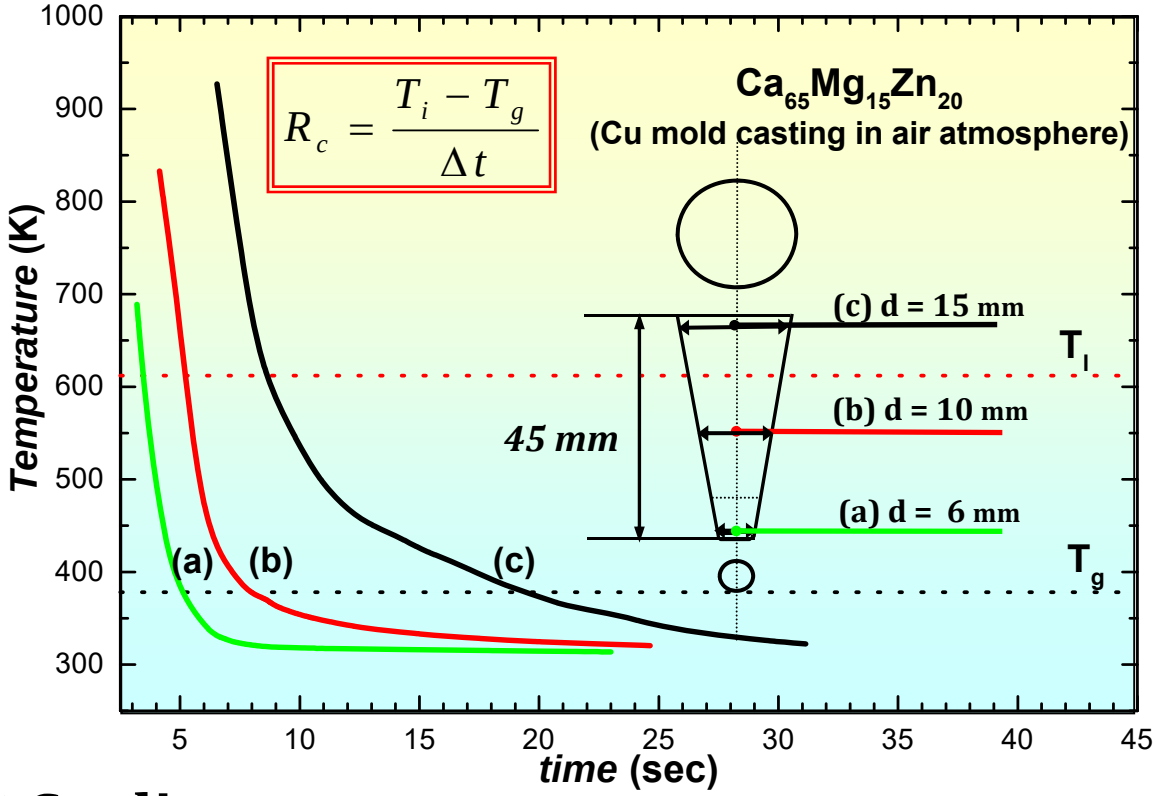


top position : 20 K/s

middle position : 93 K/s

bottom position : 149 K/s

*** Cooling curves measured at the center of the three transverse cross sections**

* J. Mater. Res. 19, 685 (2004)
* Mater. Sci. Forum 475-479, 3415 (2005)

## 3.2.3 Measurement of $R_c$

# Measurement of $R_c$ in Mg BMG ($D_{max}$=14 mm)

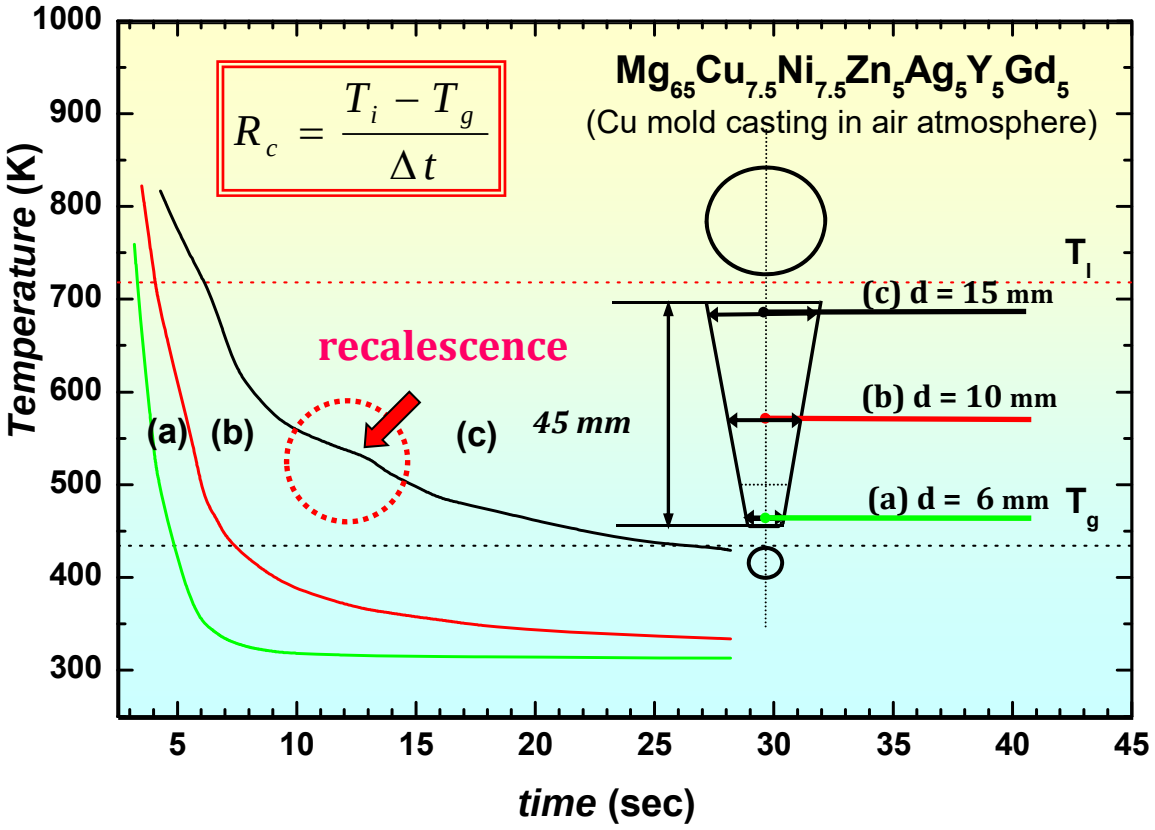


**top position : recalescence**

**middle position : 64K/s**

**bottom position : 137 K/s**

*** Cooling curves measured at the center of the three transverse cross sections**

* JAP 104, 023520 (2008)

**TABLE 3.1**

Some Representative Critical Cooling Rates ($R_c$) for Formation of Glassy Phases in Different Alloy Systems

| Alloy Composition | $R_c$ (K s$^{-1}$) | Reference |
|---|---|---|
| $Au_{77.8}Ge_{13.8}Si_{8.4}$ | $3 \times 10^6$ | [24] |
| $Ca_{60}Mg_{25}Ni_{15}$ | 24 | [25] |
| $Ca_{65}Mg_{15}Zn_{20}$ | <20 | [26] |
| $Cu_{50}Zr_{50}$ | 250 | [27] |
| $Cu_{48}Zr_{48}Al_4$ | <40 | [27] |
| $Cu_{42}Zr_{42}Ag_8Al_8$ | 4.4 | [28] |
| $Fe_{43}Cr_{16}Mo_{16}C_{10}B_5P_{10}$ | 100 | [29] |
| $Fe_{40}Ni_{40}P_{14}B_6$ (Metglas 2826) | $4.4 \times 10^7$ | [30] |
| $Hf_{70}Pd_{20}Ni_{10}$ | 124 | [31] |
| $La_{55}Al_{25}Cu_{20}$ | 58 | [32] |
| $La_{55}Al_{25}Ni_{20}$ | 69 | [32] |
| $Mg_{65}Cu_{25}Gd_{10}$ | 1 | [16] |
| $Mg_{65}Cu_{25}Y_{10}$ | 100 | [33] |
| $Mg_{65}Cu_{15}Ag_5Pd_5Gd_{10}$ | 0.7 | [34] |
| $Mg_{65}Cu_{7.5}Ni_{7.5}Ag_5Zn_5Gd_5Y_5$ | 20 | [35] |
| $Nd_{60}Co_{30}Al_{10}$ | 4 | [36] |
| $Ni_{62}Nb_{38}$ | 57 | [37] |
| $Ni_{65}Pd_{15}P_{20}$ | $10^5$ | [38] |
| $Pd_{78}Cu_6Si_{16}$ | 550 | [39] |
| $Pd_{40}Ni_{40}P_{20}$ | 128 | [22] |
| $Pd_{42.5}Cu_{30}Ni_{7.5}P_{20}$ | 0.067 | [18] |
| $Pd_{40}Cu_{25}Ni_{15}P_{20}$ | 0.150 | [18] |
| $Pd_{40}Cu_{30}Ni_{10}P_{20}$ (without fluxing) | 1.58 | [22] |
| $Pd_{40}Cu_{30}Ni_{10}P_{20}$ (with flux treatment) | 0.1 | [18] |
| $Pd_{30}Pt_{17.5}Cu_{32.5}P_{20}$ | 0.067 | [19] |
| $Pd_{82}Si_{18}$ | $1.8 \times 10^3$ | [40] |
| $Pd_{82}Si_{18}$ | 800 | [41] |
| $Pd_{81}Si_{19}$ (with flux treatment) | 6 | [42] |
| $Zr_{65}Al_{7.5}Ni_{10}Cu_{17.5}$ | 1.5 | [43] |
| $Zr_{41.2}Ti_{13.8}Cu_{12.5}Ni_{10.0}Be_{22.5}$ | 1.4 | [44] |
| $Zr_{46.25}Ti_{8.25}Cu_{7.5}Ni_{10.0}Be_{27.5}$ | 28 | [44] |
| $Zr_{57}Cu_{15.4}Ni_{12.6}Al_{10}Nb_5$ | 10 | [45] |

## 1) Effect of $B_2O_3$ fluxing

$Pd_{40}Cu_{30}Ni_{10}P_{20}$ 1.58 K s$^{-1}$ without fluxing [22]

0.1 K s$^{-1}$ with fluxing [18]

## 2) Effect of # of components

$Pd_{82}Si_{18}$ $1.8 \times 10^3$ K s$^{-1}$ ⟷ 550 K s$^{-1}$ $Pd_{78}Cu_6Si_{16}$

$Cu_{50}Zr_{50}$ 250 K s$^{-1}$ ⟷ ≤40 K s$^{-1}$ $Cu_{48}Zr_{48}Al_4$

## 3) Nature of alloying addition

$Mg_{65}Cu_{25}Y_{10}$ $Mg_{65}Cu_{25}Gd_{10}$ $Mg_{65}Cu_{15}Ag_5Pd_5Gd_{10}$

100 K s$^{-1}$ ⟷ 1 K s$^{-1}$ ⟷ 0.7 K s$^{-1}$

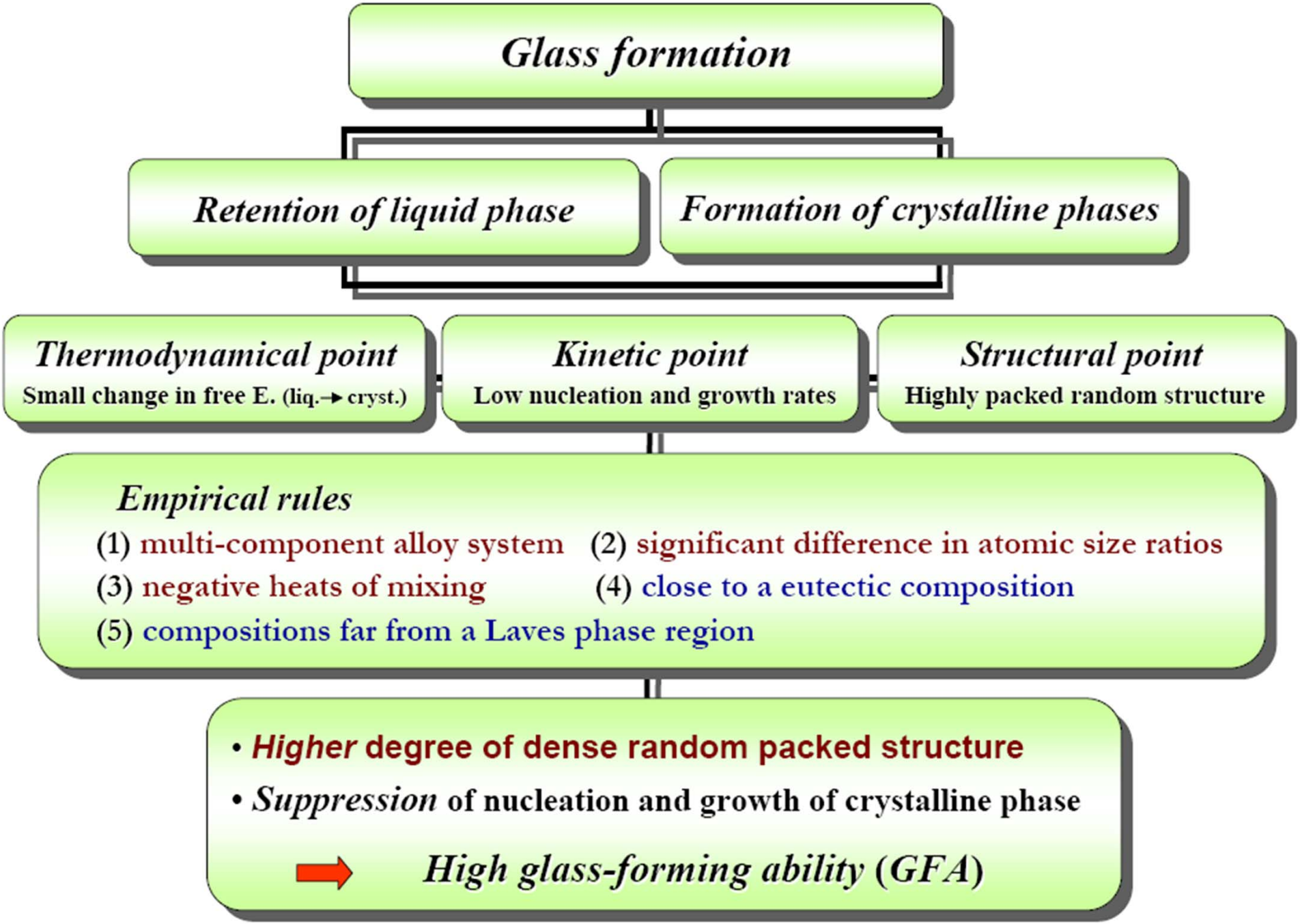
Glass formation
Retention of liquid phase
Formation of crystalline phases
Thermodynamical point
Small change in free E. (liq.→cryst.)
Kinetic point
Low nucleation and growth rates
Structural point
Highly packed random structure
Empirical rules
(1) multi-component alloy system
(2) significant difference in atomic size ratios
(3) negative heats of mixing
(4) close to a eutectic composition
(5) compositions far from a Laves phase region
• Higher degree of dense random packed structure
• Suppression of nucleation and growth of crystalline phase
High glass-forming ability (GFA)

## 3.3 Reduced Class Transition Temperature (Kinetic aspect for glass formation)

$T_{rg}$ parameter $= T_g/T_l \sim \eta$ : the higher $T_{rg}$, the higher $\eta$, the lower $R_c$

: ability to avoid crystallization during cooling

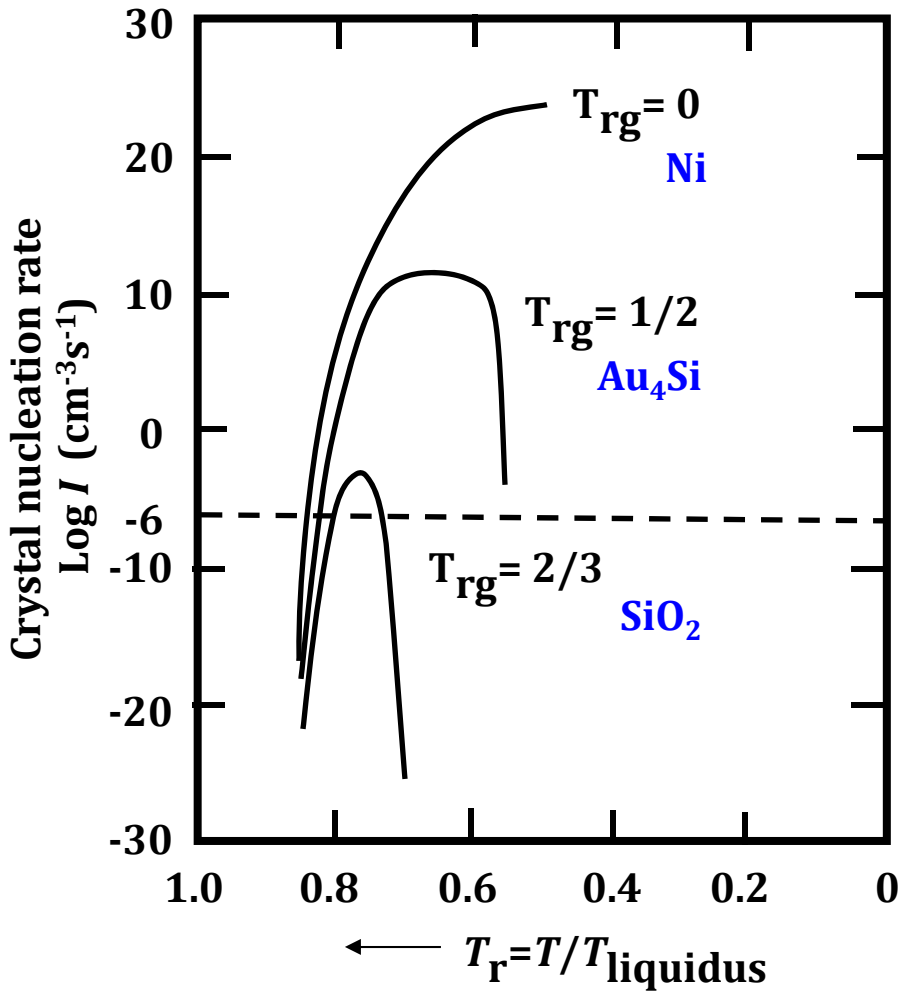


$T_{rgNi} < T_{rgAu4Si} < T_{rgSiO2}$

$R_{Ni} > R_{Au4Si} > R_{SiO2}$

*Turnbull, 1959* ff.

- **Based on the nucleation theory, Turnbull suggested that at $T_{rg} \geq 2/3$, homogeneous nucleation of the crystalline phase is completely suppressed. Most typically, a minimum value of $T_{rg} \sim 0.4$ has been found to be necessary for the glass to form.**

- **One should note the $T_l$, liquidus temperature as the point at the end of the liquid formation, and not at the beginning of melting.**

**TABLE 3.2**

Reduced Glass Transition Temperatures ($T_{rg}$) for Different Glass-Forming Alloys

| Alloy Composition | $T_{rg}$ | References |
|---|---|---|
| $Ca_{65}Al_{35}$ | 0.69 | [47] |
| $Ca_{67}Mg_{19}Cu_{14}$ | 0.60 | [48] |
| $Ca_{57}Mg_{19}Cu_{24}$ | 0.64 | [48] |
| $Cu_{65}Hf_{35}$ | 0.62 | [49] |
| $Cu_{49}Hf_{42}Al_{9}$ | 0.62 | [50] |
| $Cu_{64}Zr_{36}$ | 0.64 | [51] |
| $La_{55}Al_{25}Ni_{20}$ | 0.71 | [32] |
| $La_{62}Al_{15.5}(Cu,Ni)_{22.3}$ | 0.58 | [52] |
| $La_{50.2}Al_{20.5}(Cu,Ni)_{29.3}$ | 0.47 | [52] |
| $Ni_{62}Nb_{38}$ | 0.60 | [37] |
| $Ni_{61}Nb_{33}Zr_{6}$ | 0.49 | [53] |
| $Pd_{40}Ni_{40}P_{20}$ | 0.67 | [54] |
| $Pd_{40}Cu_{30}Ni_{10}P_{20}$ | 0.67 | [18,55] |
| $Zr_{41.2}Ti_{13.8}Cu_{12.5}Ni_{10}Be_{22.5}$ | 0.624 | [45] |
| $Zr_{45.38}Ti_{9.62}Cu_{8.75}Ni_{10}Be_{26.25}$ | 0.50 | [44] |

- The concept of $T_{rg}$ was introduced for kinetic reasons with the need to avoid crystallization [46]. It is known (and we will discuss this in some detail in Section 3.4) that $T_g$ is a very weak function of the solute content, i.e., $T_g$ varies much more slowly with solute concentration than the liquidus temperature, $T_l$. Consequently, the value of $T_{rg}$ increases with increasing solute content, up to the eutectic composition, and therefore it becomes easier to avoid crystallization of the melt at the eutectic composition [13]. This reasoning seems to work well in simple binary alloy systems. But, in the case of multicomponent alloy systems such as the BMG compositions, the values of $T_g$ and $T_l$ vary significantly. Since the variation of viscosity with temperature is different for different alloy systems (and depends on whether a glass is strong or fragile), $T_g$ alone may not provide information about the variation of viscosity with temperature and therefore, the $T_{rg}$ criterion may not be valid in some systems.

Easy glass formation at compositions corresponding to high $T_{rg}$ can be easily realized in alloy systems that feature deep eutectic reactions in their phase diagrams, and this is further explained in Section 3.4.

## 3.4 Deep Eutectics (Thermodynamic aspect for glass formation)

- **High GFA : low free energy** $\Delta G(T)$

  **for transformation of liquid to crystalline phase**

$$\Delta G(T) = \Delta H_f - T\Delta S_f$$

$\Delta G \downarrow \rightarrow \Delta H_f \downarrow$ & $\Delta S_f \uparrow$

Enthalpy of fusion — Entropy of fusion

$\Delta S_f \uparrow$ : **proportional to the number of microscopic states**

Entropy of fusion

**Multi-component alloy systems** containing more than 3 elements

*causes an increase in the degree of dense random packing*

$\Delta H_f \downarrow$ **Large negative enthalpy of mixing** among constituent elements

Enthalpy of fusion

* **The free energy at a constant temperature also decreases in the cases of low chemical potential caused by low enthalpy and high reduced glass transition temperature (=$T_l/T_g$) and high interface energy between liquid and solid phase.**

## 3.4 Deep Eutectics (Thermodynamic aspect for glass formation)

$\Delta H_f$ ↓ → **deep eutectic condition: increase stability of stable liquid (= $T_g/T_l$ ↑)**

**- decreasing melting point → less supercooled at $T_g$ → $\Delta G = G^{liq} - G^{cryst}$ ↓**

**ex) metallic / inorganic system**

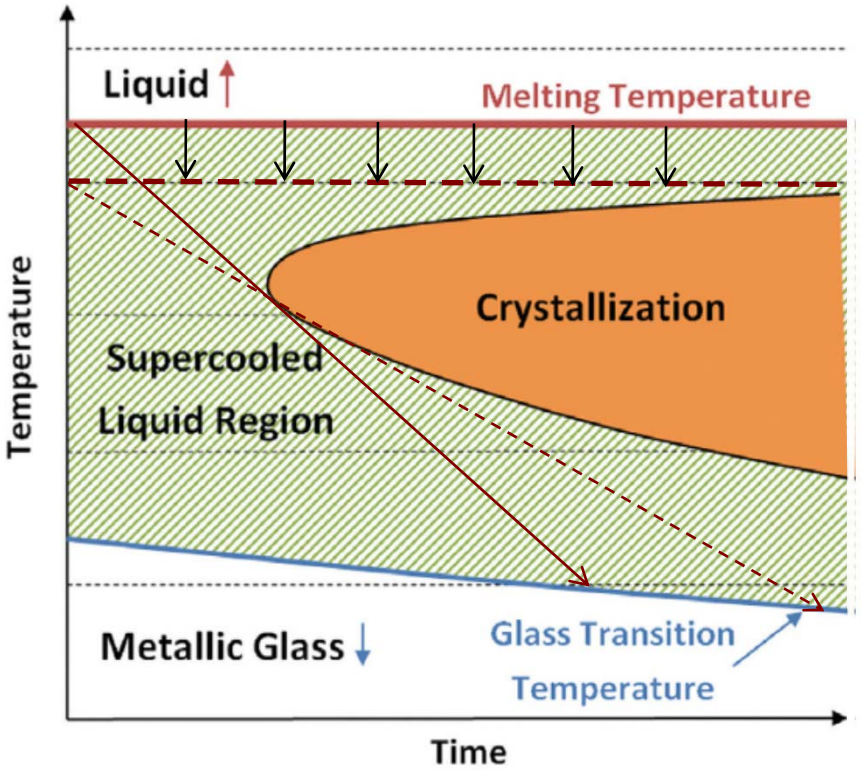


**Glass forming region:**
**Compositions near the eutectic**

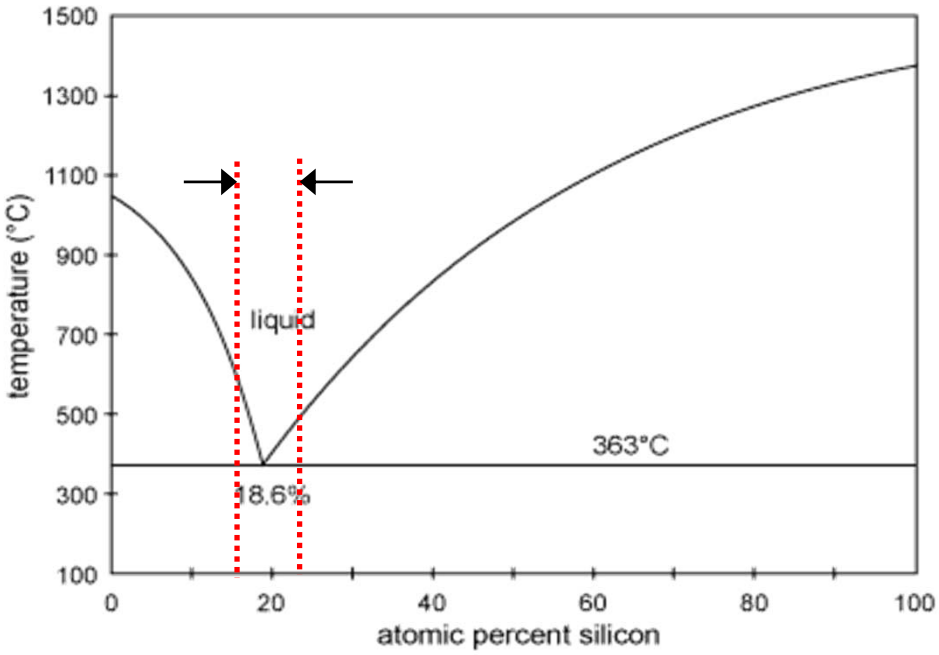

# Multi-component eutectic alloys with strong negative heat of mixing

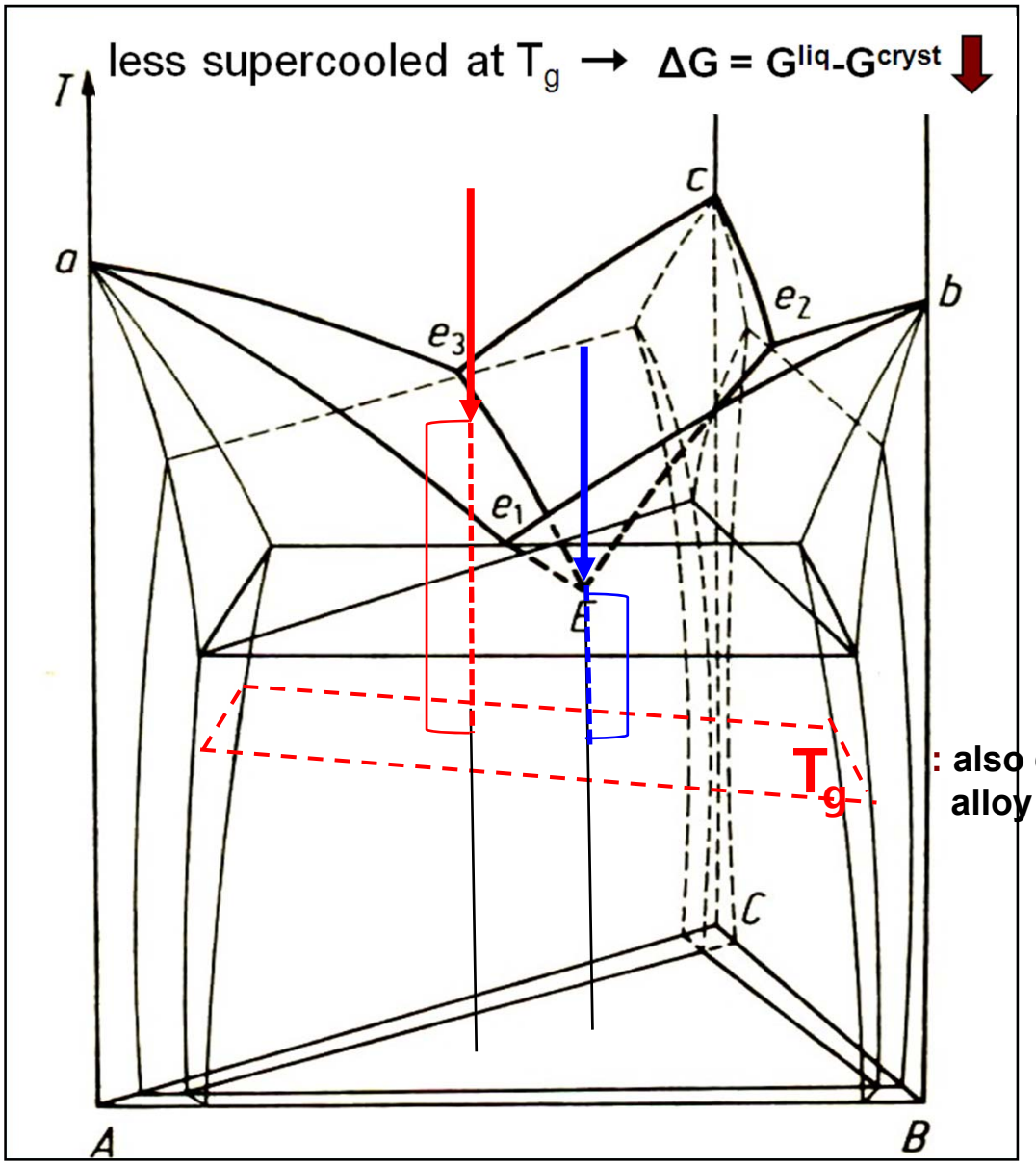


: also changes depending on alloy composition

P. Haasen, Physical Metallurgy 3rd ed

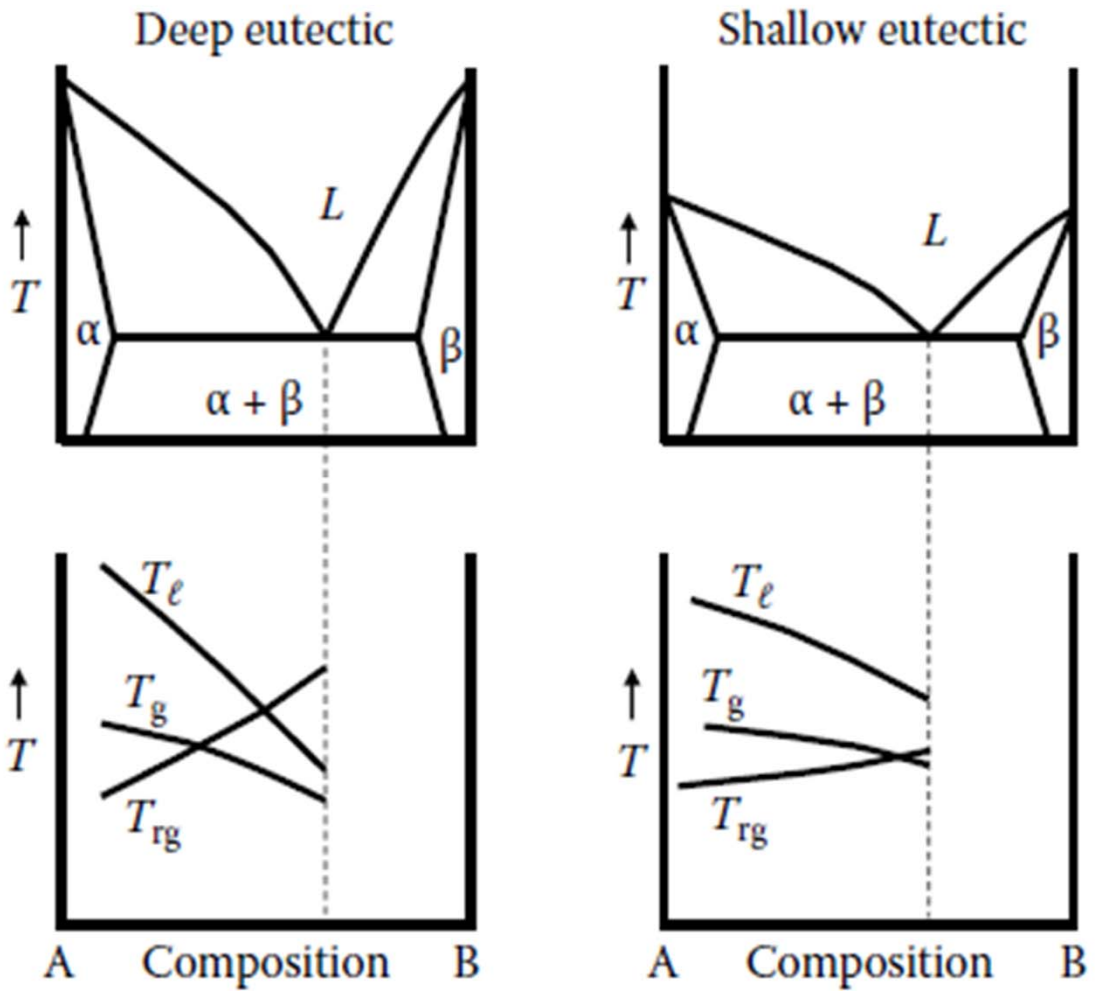


**$T_{rg}$~ highest value at eutectic composition**

**$T_{rg}$~ may not be high at eutectic composition**

**FIGURE 3.3**

Schematic variation of the glass transition temperature, $T_g$, liquidus temperature, $T_\ell$, the reduced glass transition temperature, $T_{rg}$, in two different types of eutectic systems—deep eutectic and shallow eutectic.

Ribbons of about 20–50 µm in thickness were produced by melt-spinning techniques in a number of binary alloy systems near eutectic compositions and they were confirmed to be glassy. Some of the most investigated eutectic compositions are found in Fe–B, Pd–Si, Cu–Zr, Ni–Nb, Ni–Ta, etc., alloy systems [1,2]. There have been some reports in recent years of "bulk" (?) metallic glass synthesis in binary alloy systems such as Ca–Al [59], Cu–Hf [49], Cu–Zr [51], Ni–Nb [37], and Pd–Si [42]. But, the maximum diameters of these binary alloy glassy rods were only 1 or 2 mm, and even then, some of these alloy glasses contained nanocrystalline particles embedded in the glassy matrix [60]. This point will be further discussed in detail in later chapters. But, the important point here is that the "bulk" glassy phase is produced not at the eutectic composition, but, at off-eutectic compositions. Further, the highest GFA, i.e., the composition at which glass formation was the easiest or the maximum diameter of the BMG rod could be obtained, was located away from the eutectic composition. The best glass-forming compositions have been reported to be at 35 at.% Hf in Cu–Hf, 36 at.% Zr in Cu–Zr, 38 at.% Nb in Ni–Nb, and 19 at.% Si in Pd–Si alloy systems. But, the eutectic compositions in these alloy systems are at 33.0 and 38.6 at.% Hf in Cu–Hf, 38.2 at.% Zr in Cu–Zr, 40.5 at.% Nb in Ni–Nb, and 17.2 at.% Si in Pd–Si systems [61]. Similarly, it was reported that while a nearly fully glassy rod with 12 mm diameter could be obtained at an off-eutectic composition near $La_{62}Al_{15.7}(Cu,Ni)_{22.3}$, only a 1.5 mm diameter rod could be obtained in a fully glassy condition for the eutectic alloy of $La_{66}Al_{14}(Cu,Ni)_{20}$ [52].

# Strategy for pinpointing the best glass-forming alloys

**Upon cooling, a melt freezes into a glass a $T_g$ if the crystal nucleation can be avoided altogether. But even when heterogeneous nucleation occurs as in most practical cases, a glass can still form if the growth of the nucleation is suppressed. This scenario has been verified by observing the effects of quenched-in-nuclei on the formation of Al-based amorphous alloys. The consideration of diminished crystal growth at high undercoolings, as well as the use of TTT diagrams by treating glass formation as avoiding both nucleation and growth of crystals, all justify the premise for our derivation: 1) the competition between glass formation and crystalline phase growth controls GFA, And 2) a glass will form if its $T_g$ isotherm is higher than the growth temperature of any of the possible crystalline phases.**

# Strategy for pinpointing the best glass-forming alloys

- Condition for the glass formation
  - No crystal nucleation
  - suppress growth of the nuclei

➡ "$T_g$ > growth temperature of any of the possible crystalline phases"

- Growth/Tip temperature of i crystalline phase, $T_i^x$

= Thermodynamic equilibrium temp. − undercooling required for growth

- Upon cooling, the phase having the highest $T_i^x$ is kinetically the most stable one.

➡ $T_g \geq T_i^x (x = eu, \alpha, \beta, \ldots)$

$$T_g \geqslant T_i^{eu}, \quad T_g \geqslant T_i^{\alpha}, \quad \text{and } T_g \geqslant T_i^{\beta}$$

: "Condition for Glass formation"

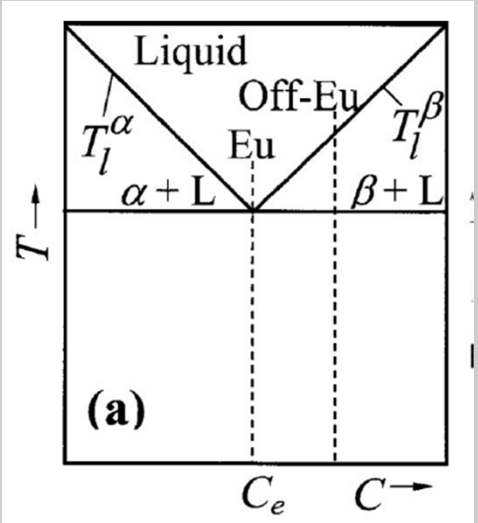

# Glass-forming condition by controlling growth: Symmetric eutectic

- $T_i^x$: function of $V$ (growth rate)

$$T_i^{eu} = T_e - K_e V^{1/2},$$

$$T_i^{\alpha} = T_l^{\alpha} - \frac{GD}{V} - K_{\alpha} V^{n},$$

$$T_i^{\beta} = T_l^{\beta} - \frac{GD}{V} - K_{\beta} V^{n},$$

*G*: Temp. gradient
*K*: growth constant

*Negligible G effects at high V*

- Glass-forming zone →

$$V \geq V_c^{e} \text{ when } C_0^{\min} \leq C \leq C_0^{\max}, \quad T_i^{eu} = T_g, V = V_c^{e}$$

$$V \geq V_c^{\alpha} \text{ when } C < C_0^{\min}, \quad T_i^{\alpha} = T_g, V = V_c^{\alpha}$$

$$V \geq V_c^{\beta} \text{ when } C > C_0^{\max}, \quad T_i^{\beta} = T_g, V = V_c^{\beta}$$

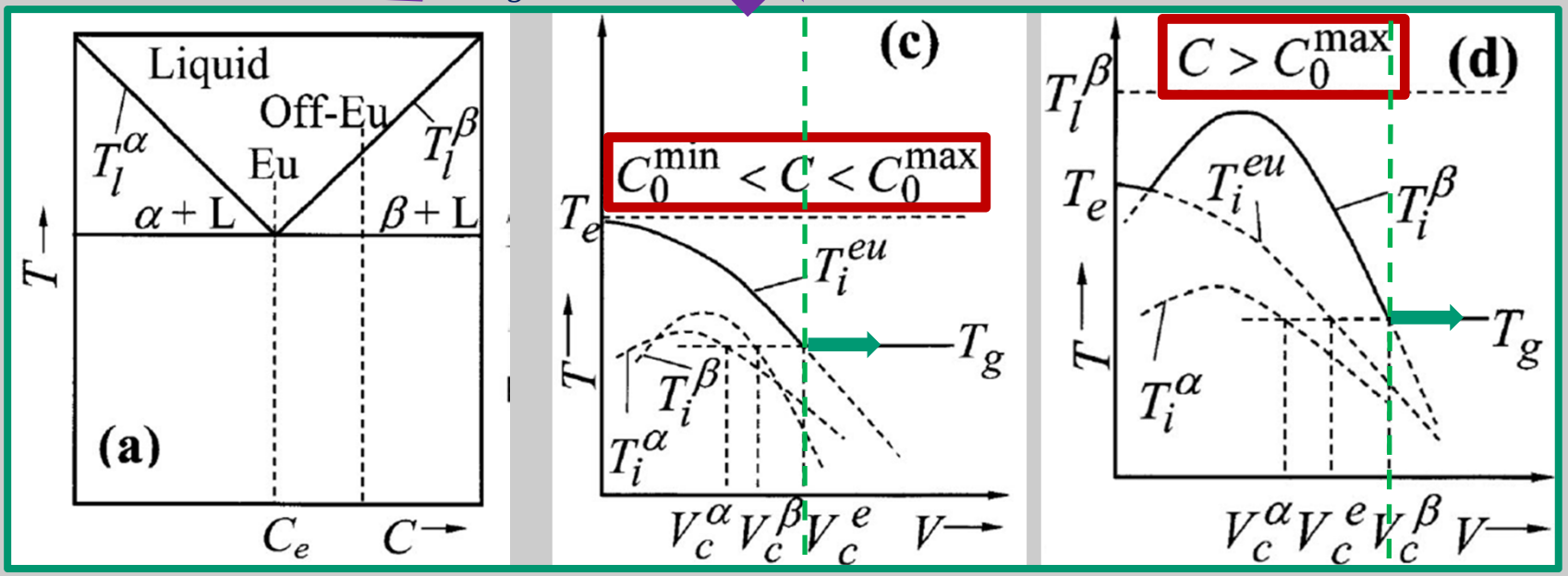

# Glass-forming condition by controlling growth: Symmetric eutectic

$$V_c^e = \frac{(T_e - T_g)^2}{K_e^2},$$ **independent to composition**

$$V_c^\alpha = \frac{[m_\alpha(C - C_e) + T_e - T_g]^{1/n}}{K_\alpha^{1/n}},$$

$$V_c^\beta = \frac{[m_\beta(C - C_e) + T_e - T_g]^{1/n}}{K_\beta^{1/n}},$$

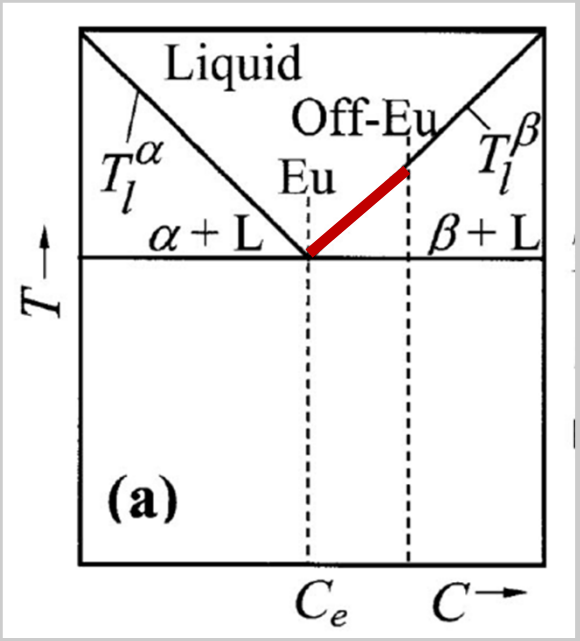


$$\frac{T_l^\alpha - T_e}{C - C_e} = m_\alpha \text{(<0)}$$

$$\frac{T_l^\beta - T_e}{C - C_e} = m_\beta \text{(>0)}$$

$$C_0^{\min} = C_e + \frac{(T_e - T_g)}{m_\alpha \text{(<0)}}\left[\frac{K_\alpha}{K_e^{2n}}(T_e - T_g)^{2n-1} - 1\right]$$

$$C_0^{\max} = C_e + \frac{(T_e - T_g)}{m_{\beta\text{(>0)}}}\left[\frac{K_\beta}{K_e^{2n}}(T_e - T_g)^{2n-1} - 1\right]$$

$V_c^e =$ **Lowest critical growth rate for full glass formation**

- $C_0^{\min} \le C \le C_0^{\max}$ region
  - ➡ Best GFA
- **Easy glass former**
  - ➡ **Δ** ($T_g - T_e$) = small or large $K_e$

**Regular eutectic system**

$$C_0^{min} < C_e < C_0^{max}$$

$$K_e < K_\alpha^{1/2n}(T_e - T_g)^{(1-1/2n)}$$

$$K_e < K_\beta^{1/2n}(T_e - T_g)^{(1-1/2n)}$$

Relative easy growth of eutectic

**Part of a regular eutectic phase diagram**

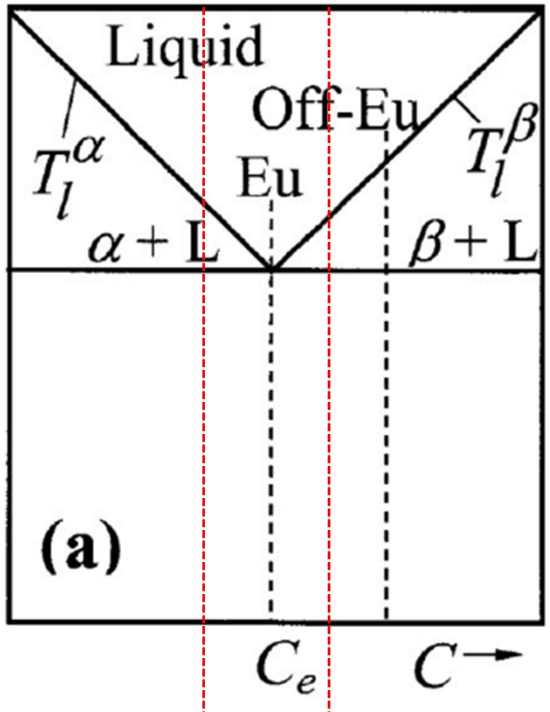


**Glass-forming and Composite-forming Zones (symmetrical about eutectic composition)**

**Omitting the Negligible G effects at high V, a glass-forming zone: growth rate range over which a given alloy with composition C becomes a glass.**

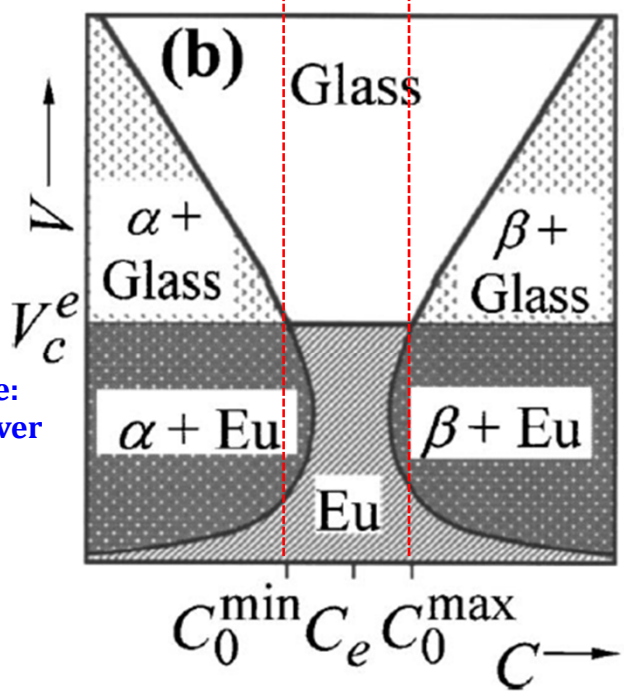


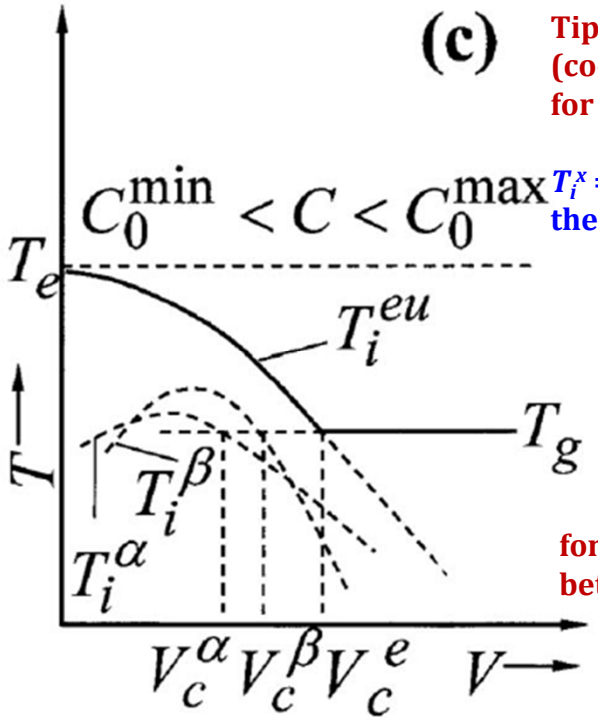


**Tip temp.-growth rate (cooling rate) relationship for eutectic, dendritic α, β**

**$T_i^x$ = growth/tip temp. of the i crystalline phase**

**for alloy composition between $C_0^{min}$ and $C_0^{max}$**

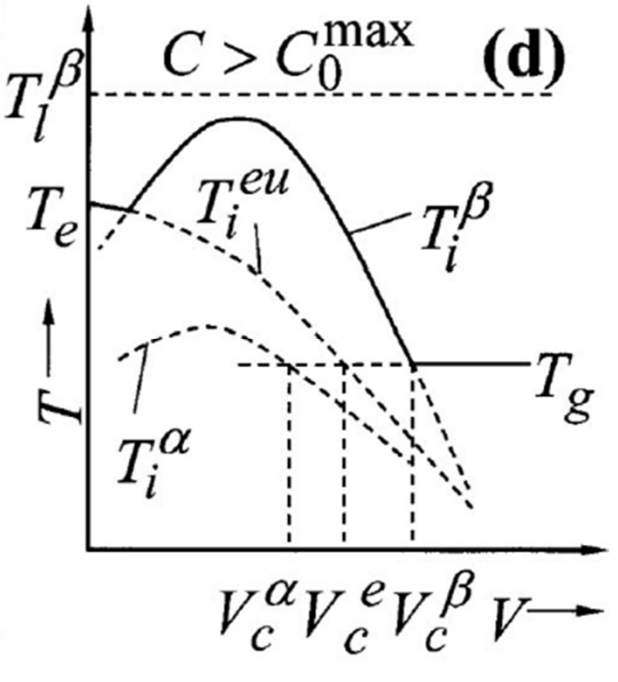


**for alloy composition of $C > C_0^{max}$**

$$C_e \le C_0^{min} \le C_0^{max}$$

$$K_\alpha^{1/2n}(T_e - T_g)^{(1-1/2n)} < K_e < K_\beta^{1/2n}(T_e - T_g)^{(1-1/2n)}$$

Relative easy growth of α growth (and/or the greater difficulty of β growth)

**Part of a irregular eutectic phase diagram**

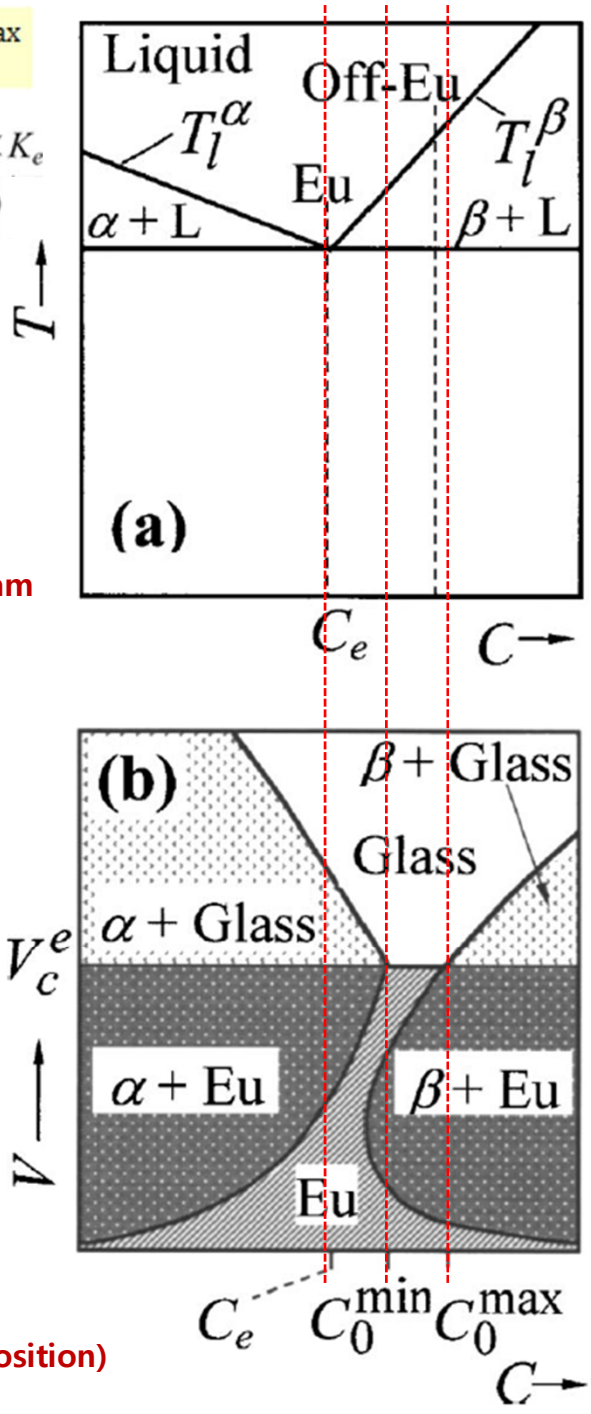


**Tip temp.-growth rate (cooling rate) relationship for eutectic, dendritic α, β**

**for alloy composition of $C < C_0^{min}$**

**for alloy composition between $C_0^{min} < C < C_0^{max}$**

**Glass-forming and Composite-forming Zones (asymmetrical about eutectic composition)**

**Schematic diagram showing skewed eutectic coupled zone and its relation to the glass-forming ability**

A eutectic system with skewed coupled zone

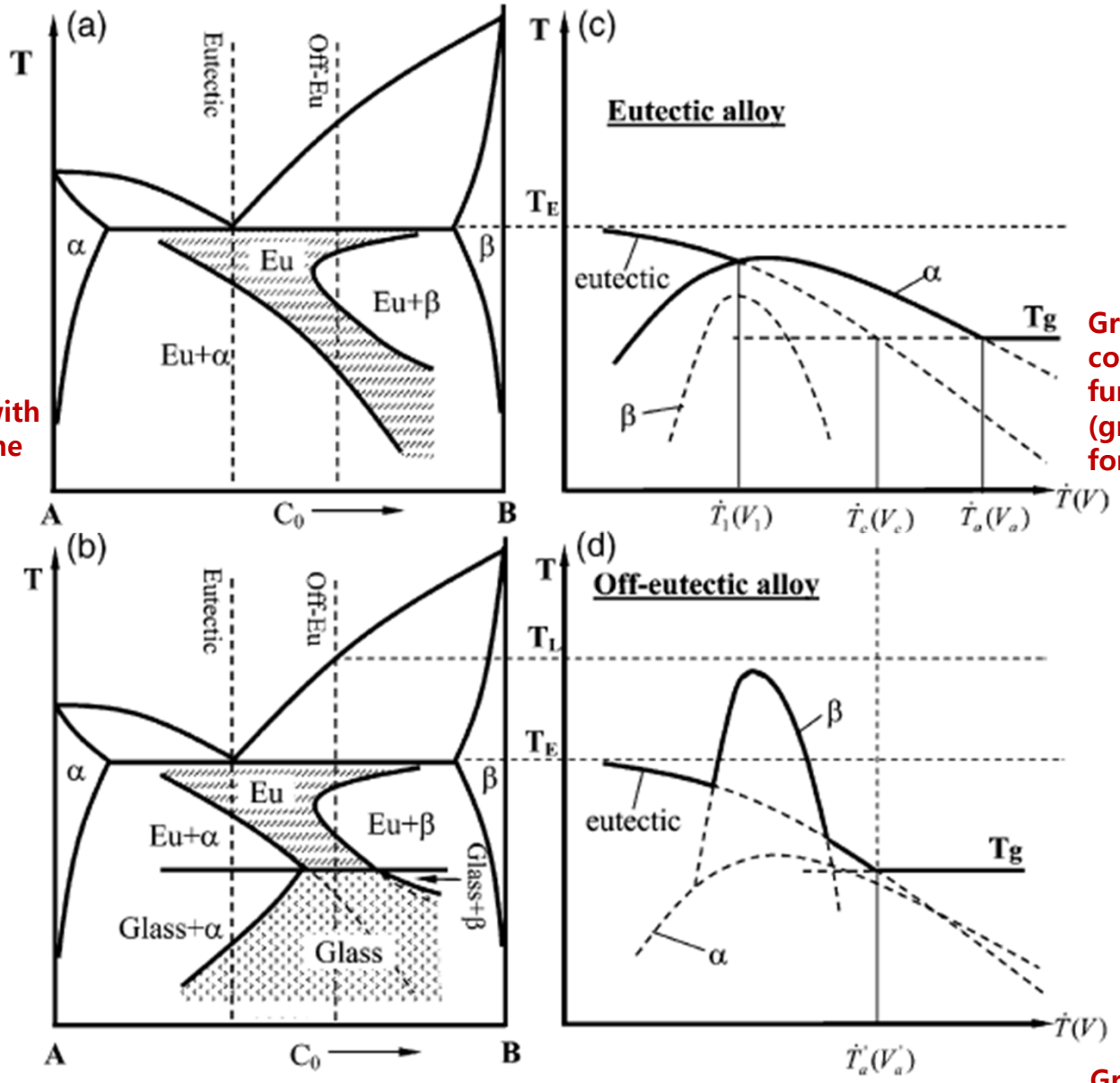


Growth temp. of the constituents as a function of cooling rate (growth rate) for the eutectic alloy

Glass forming and composite forming regions related to the skewed coupled zone

Growth temp. of the constituents as a function of CR (GR) for an off-eutectic alloy

# Composites & Glass forming composition

< Symmetric Eutectic>

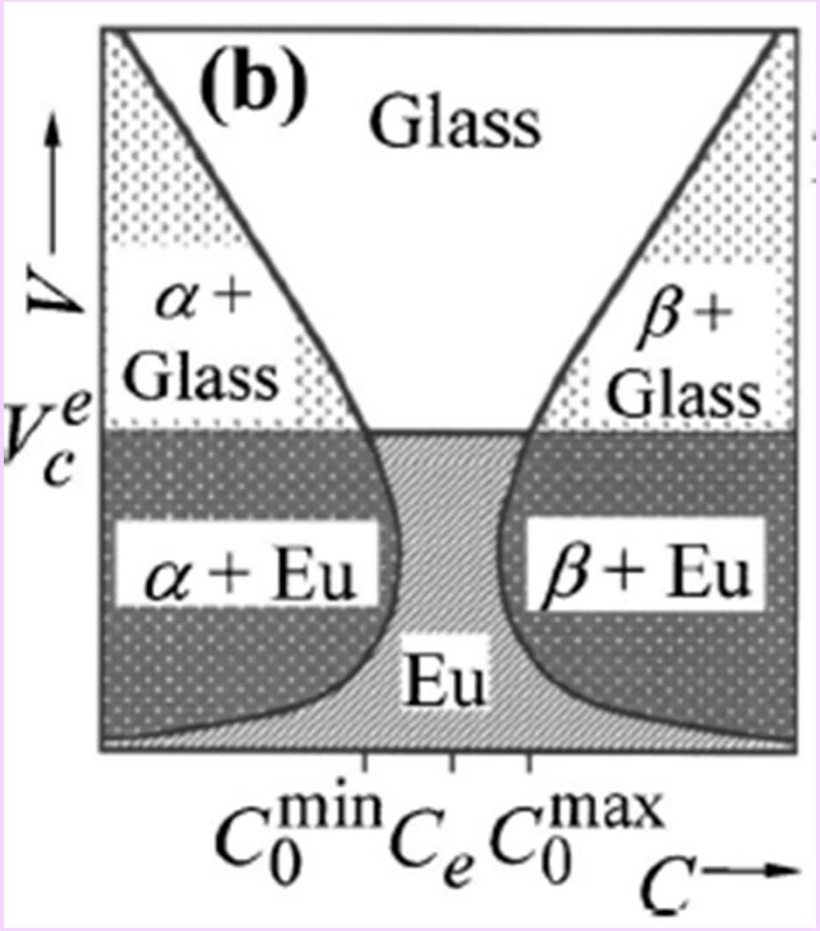


< Non-symmetric Eutectic>

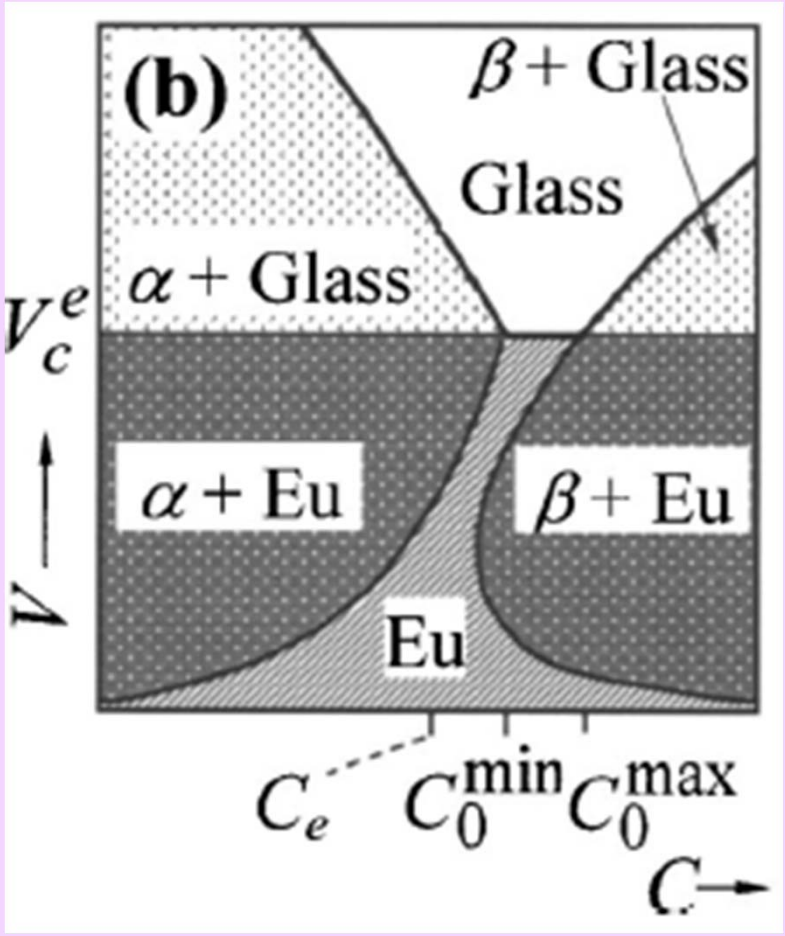


- **Glass region is located between composites with different 2nd phases.**

➡ **Useful to find the composition with maximum GFA**

# Composites & Glass forming composition

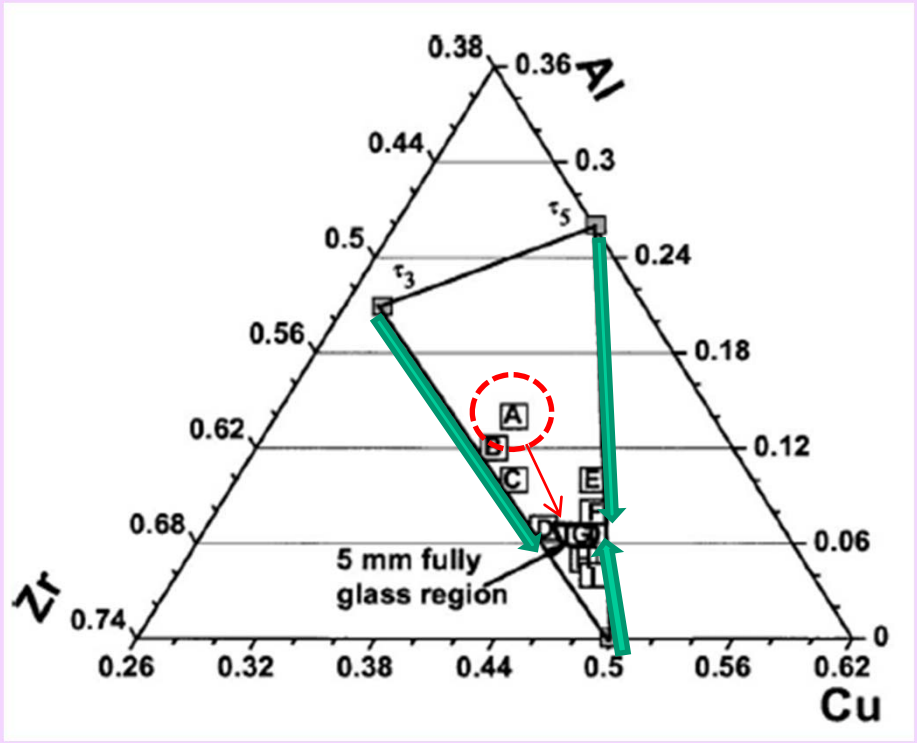


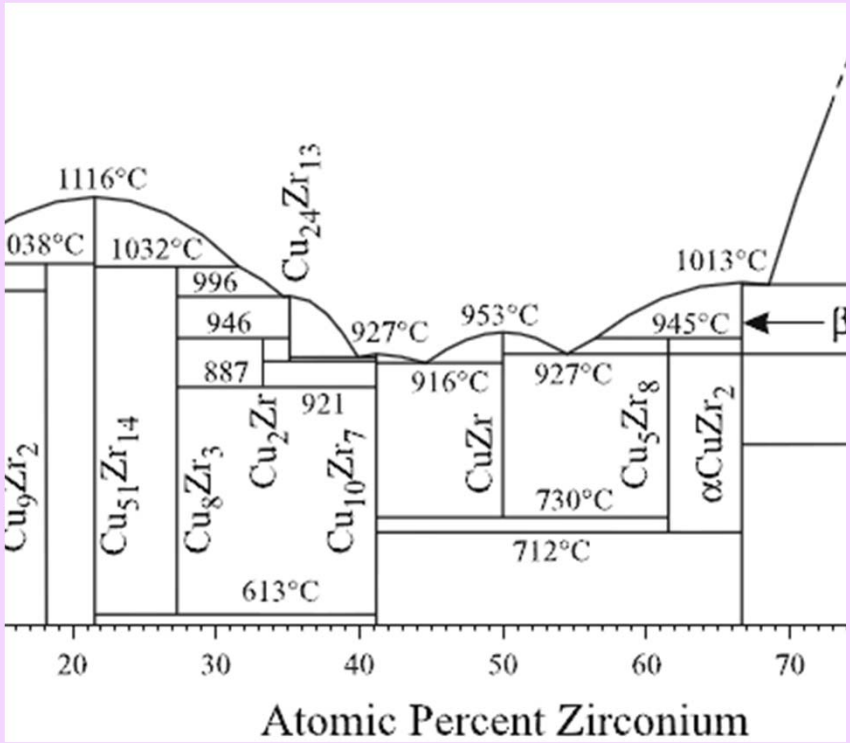


- Tie triangle among ZrCu, $\tau_3$ , $\tau_5 \rightarrow$ A = "ternary eutectic composition"

1. A($Zr_{48}Cu_{38}Al_{14}$) : eutectic composition but glass and composite X

➡ In Cu-Zr alloy, the composition with high GFA is moved to near liquidus line with higher slope of Zr-rich composition.

# Composites & Glass forming composition

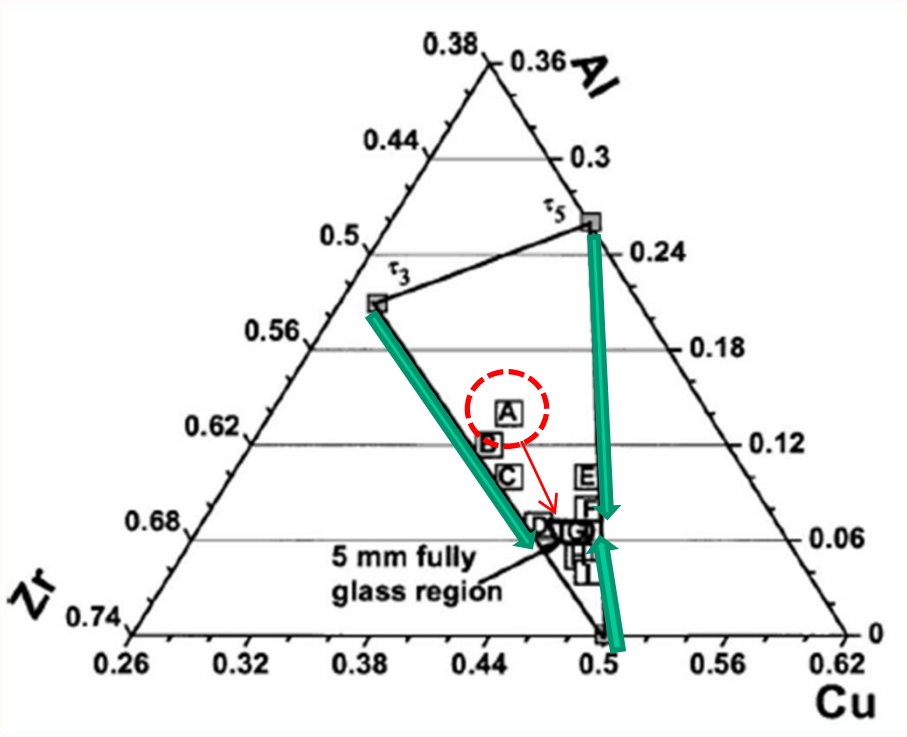


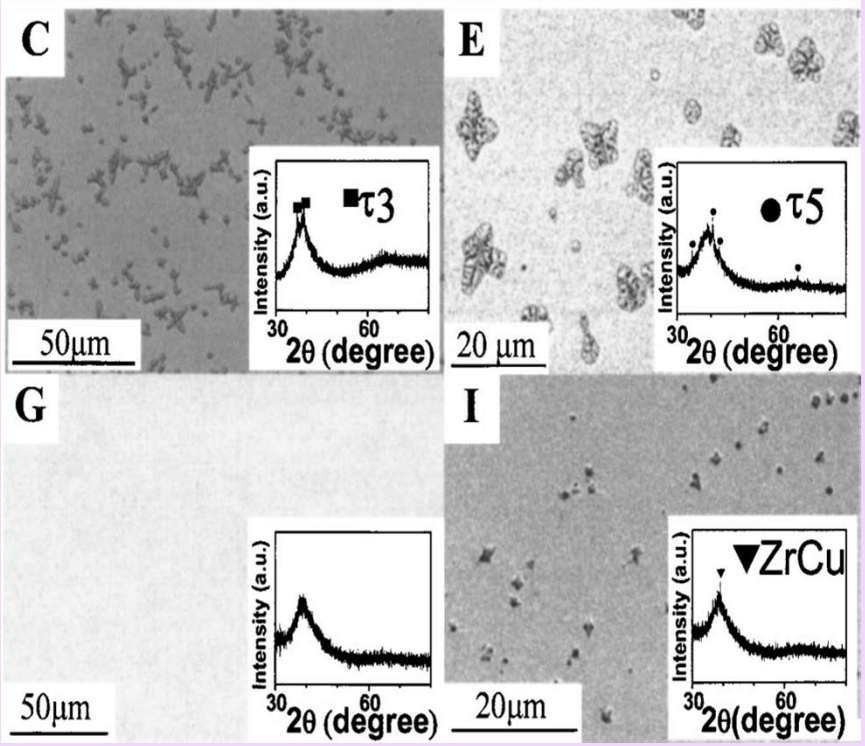


**2.Three composition forming region (casted into 5 mm-diam copper mold)**

**Following arrows, $\tau_3$ +glass (B,C,D), $\tau_5$ + glass (E,F), ZrCu + glass (I,H) ~**

➡ **At point G, competing crystalline phase changes**

➡ **G = Formation of fully glass**

## 3.5 Topological Model (Structural aspect for glass formation)

Metallic glasses produced by RSP methods in the form of thin ribbons have been traditionally classified into two groups, viz., metal–metalloid and metal–metal types. Structural models of the metal-metalloid-type metallic glasses have identified that the best composition to form a glass is one that contains about 80 at.% of the metal component and 20 at.% of the metalloid component. The actual glass composition ranges observed are 75–85 at.% of the metal and 15–25 at.% of the metalloid. As stated in Chapter 2, the 80 at.% of the metal can be either a single transition metal or a combination of transition metals or one or a combination of noble metals. Similarly, the 20 at.% of the metalloid content could be made up of just one component or a mixture of a number of components. In the case of metal-metal types, however, there is no such restriction on compositions. Metal-metal-type metallic glasses have been observed to form over a wide range of compositions, starting from as low as 9 at.% of solute. Some typical compositions in which metal-metal type glasses have been obtained are $Cu_{25–72.5}Zr_{27.5–75}$, $Fe_{89–91}Zr_{9–11}$, $Mg_{68–75}Zn_{25–32}$, $Nb_{55}Ir_{45}$, and $Ni_{58–67}Zr_{33–42}$ [65].

# * Metallic glass : Randomly dense packed structure

**1) Atomic size difference: TM – metalloid (M, ex) Boron)**

→ **M is located at interior of the tetrahedron of four metal atoms ($TM_4M$)**

→ **denser ⇨ by increasing resistivity of crystallization, GFA ⇧**

→ **Ex) Fe-B: tetrahedron with B on the center position**

**1) interstitial site, B= simple atomic topology**

**2) skeleton structure**

**3) bonding nature: close to covalent bonding**

Irrespective of the actual size of the voids and whether the above model is valid or not, it is of interest to note that the metal-metalloid-type binary phase diagrams exhibit deep eutectics at around a composition of 15–25 at.% metalloid. Some typical examples are Fe–B (17 at.% B), Au–Si (18.6 at.% Si), and Pd–Si (17.2 at.% Si). Therefore, the concepts of deep eutectics and structural models also seem to converge in obtaining glasses in the (transition or noble) metal-metalloid types.

### 3.5.2. Egami and Waseda Criterion

One of the possible ways by which a crystalline metallic material can become glassy is by the introduction of lattice strain. The lattice strain introduced disturbs the crystal lattice and once a critical strain is exceeded, the crystal becomes destabilized and becomes glassy. In fact, Egami takes pains to state that "In general, alloying makes glass formation easier, not because alloying stabilizes a glass, but because it destabilizes a crystal" [72, p. 576]. Using the atomic scale elasticity theory, Egami and Waseda [73] calculated the atomic level stresses in the solid solution (the solute atoms are assumed to occupy the substitutional lattice sites in the solid solution) and the glassy phase. They observed that in a glass, neither the local stress fluctuations nor the total strain energy vary much with solute concentration, when normalized with respect to the elastic moduli. But, in a solid solution, the strain energy was observed to increase continuously and linearly with solute content. Thus, beyond a critical solute concentration, the glassy alloy becomes energetically more favorable than the corresponding crystalline lattice. From the vast literature available on the formation of binary metallic glasses obtained by RSP methods, the authors noted that a minimum solute concentration was necessary in a binary alloy system to obtain the stable glassy phase by RSP methods.

## 2) min. solute content, $C_B^*$: empirical rule By Egami & Waseda: in A-B binary system

$$C_B^{min}\left|\frac{(v_B - v_A)}{v_A}\right| = C_B^{min}\left|\left(\frac{r_B}{r_A}\right)^3 - 1\right| \approx 0.1$$

ν: atomic volume
A: matrix, B: solute

minimum concentration of B for glass formation 존재

→ Inversely proportional to atomic volume mismatch

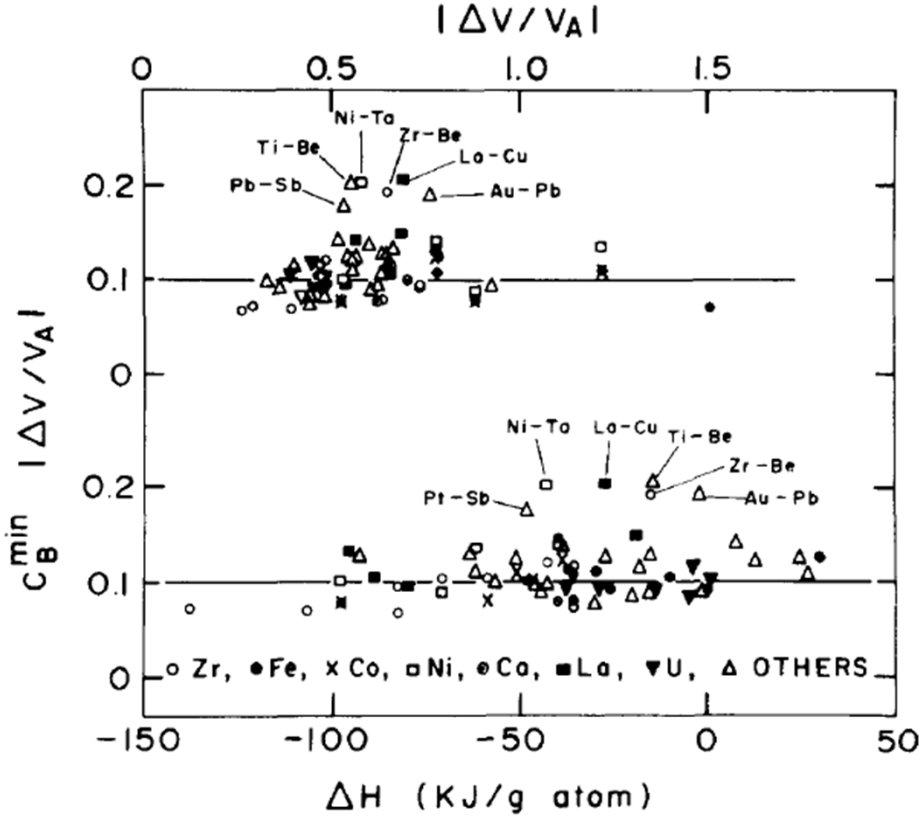


Fig. 1. Relation between $|\lambda_0| = C_B^{min}\,|\Delta v/v_A|$, and $|\Delta v/v_A|$ and $\Delta H$, for 66 binary systems which can be vitrified by liquid quenching.

## 3.5.3. Nagel and Tauc Criterion

Nagel and Tauc [74,75] proposed that a glass is most likely to form if its electronic energy lies in a local metastable minimum with respect to composition change. They showed that if the structure factor corresponding to the first strong peak of the diffuse scattering curve, $K_p$, satisfies the relationship $K_p = 2\,k_F$, where $k_F$ is the wave vector at the Fermi energy, then the electronic energy does indeed occupy a local minimum.

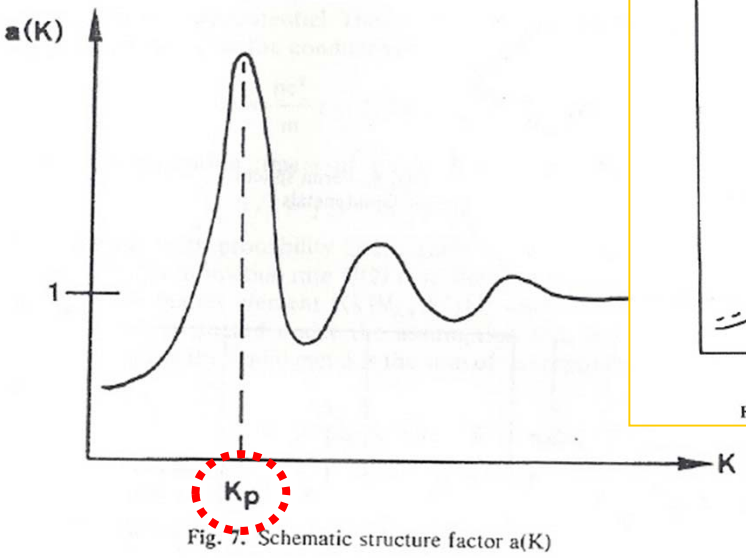

Fig. 7. Schematic structure factor a(K)

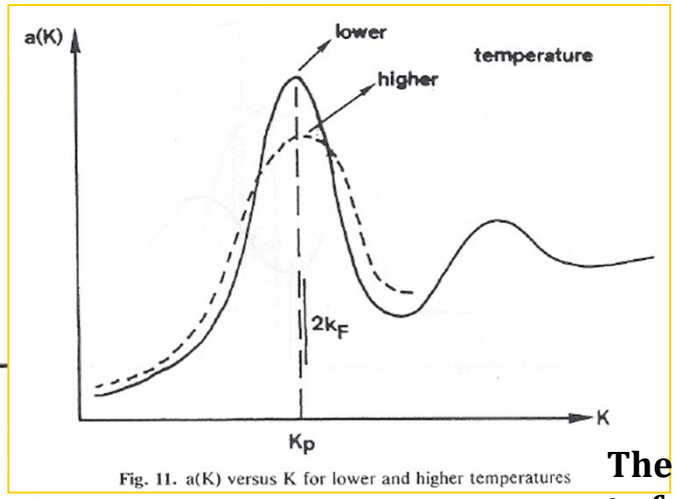

Fig. 11. a(K) versus K for lower and higher temperatures

**Kp = 2 $k_F$**

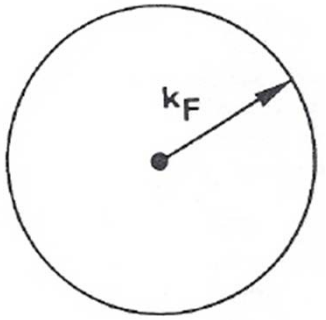


**The conduction electrons are suppose to form a degenerate free-electron gas with a spherical Fermi surface.**

$$2K_F = 2(3\pi^2 n)^{1/3} = 2\left(\frac{3\pi^2}{eR_H}\right)^{1/3}$$

**a(K) Fourier transform of the pair correlation function g(r)**

**Kp Nearest neighbor distance of the liquid metal in K-space**

**: Diameter of Fermi surface**